New insight into device therapy for chronic heart failure

Ypenburg, C.

Chapter 9

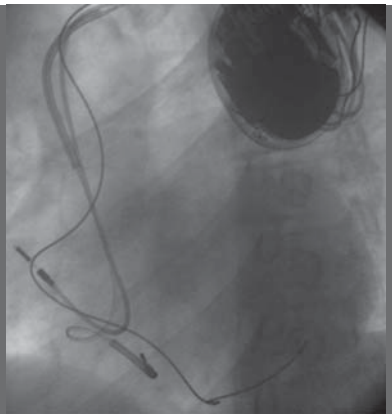

Non-invasive imaging in cardiac resynchronization therapy – part 1: selection of patients

Claudia Ypenburg
Jos J. Westenberg
Gabe B. Bleeker
Nico R. Van de Veire
Nina Ajmone Marsan
Maureen M. Henneman
Ernst E. van der Wall
Martin J. Schalij
Theodore P. Abraham
S. Serge Barold
Jeroen J. Bax

PACE 2008; in press

ABSTRACT

Cardiac resynchronization therapy (CRT) is an established therapy for patients with advanced heart failure, depressed left ventricular function and wide QRS complex. However, individual response varies, and a substantial amount of patients do not respond to CRT. Recent studies observed that assessment of inter- and particularly intraventricular dyssynchrony may allow identification of potential responders to CRT. In addition, presence of scar tissue and venous anatomy may play a role in the selection of candidates. In this review, an extensive overview of the available dyssynchrony measurements is provided using echocardiography as well as magnetic resonance imaging (MRI) and nuclear imaging. Furthermore, other information derived from MRI, nuclear imaging and computed tomography useful for the selection of potential candidates for CRT will be discussed.

INTRODUCTION

Cardiac resynchronization therapy (CRT) is an effective treatment for patients with end-stage drug-refractory heart failure (HF), depressed left ventricular (LV) function and wide QRS complex as demonstrated in various large multi-center trials. CRT has a beneficial effect on HF symptoms, exercise capacity, LV function, HF hospitalization and mortality rates (1-6). Based on the available evidence, the American College of Cardiology/American Heart Association/ Heart Rhythm Society guidelines consider end-stage HF as a class I indication for CRT according to the following selection criteria (7):

- New York Heart Association (NYHA) class III or IV despite maximal therapy
- LV ejection fraction (EF) <35%
- QRS duration >120 ms

Despite the impressive results of CRT in the large clinical trials, a consistent percentage of patients failed to benefit when the above criteria were used, the so-called "non-responders". The prevalence of responders is around 70% when clinical end-points are used (e.g. improvement in NYHA class, Table 1A), but can be much lower when echocardiographic end-points are used. Most studies used a cut-off value for substantial reverse remodeling of 10% or 15%. Using these cut-off values the response rate after CRT in terms of reverse remodeling lies between 44% and 62% (Table 1B).

Response to CRT has been related to the presence of cardiac dyssynchrony prior to implantation. Patients with HF can exhibit dyssynchrony at different levels, which can be (partially) corrected by CRT (8):

- Interatrial dyssynchrony, reflecting dyssynchronous contraction between the right and left atrium (9)
- Atrioventricular (AV) dyssynchrony, resulting in reduced LV filling time,
- Interventricular dyssynchrony, resulting in dyssynchronous contraction between the left and right ventricle (RV),
- LV (or intraventricular) dyssynchrony, reflecting contraction delay within the LV
- Intramural dyssynchrony, reflecting heterogenous LV activation patterns with differing location and extents of specific ventricular delays (10)

A variety of techniques have been proposed to quantify cardiac dyssynchrony in HF patients, ranging from QRS duration to more sophisticated echocardiographic techniques such as 3-dimensional (3D) echocardiography and strain (rate) imaging. Non-echocardiographic imaging techniques have also been advocated to assess LV dyssynchrony such as magnetic resonance imaging (MRI) and nuclear imaging. Currently, echocardiography is considered the optimal method and it has been demonstrated that the presence of LV dyssynchrony is the dyssynchrony parameter that is most predictive for CRT response.

Besides lack of dyssynchrony, other factors may prohibit CRT response. Several imaging techniques may provide additional information on suboptimal lead positioning, scarred and viable myocardium, and venous anatomy.

In this review (part 1), the value of echocardiography and other non-invasive imaging techniques for selection of CRT candidates will be discussed. In part 2, the role of imaging techniques for follow-up of CRT patients and optimization of pacemaker settings after device implantation will be addressed.

Table 1A. Clinical response rates (expressed as improvement in NYHA class) in 15 currently largest observational and randomized CRT studies

Authors	No. of patients	Follow-up (mo)	Ischemic etiology (%)	NYHA class	QRS duration (ms)	LVEF (%)	Response rate (%)
Abraham et al. (3)	228	6	50	3.1±0.3	167±21	22±6	68
Gasparini et al. (100)	104	±9	55	3.0±0.7	165±37	27±7	69
Higgins et al. (101)	245	6	67	2.9±0.7	160±27	21±6	74
Young et al. (4)	187	6	64	3.1±0.3	165±22	24±7	±70
Bristow et al. (5)	1212	6	54	3.1±0.3	160	21	59
Molhoek et al. (102)	125	6	54	3.1±0.3	176±25	23±8	79
Bleeker et al. (103)	170	6	55	3.2±0.4	173±27	21±8	78
Leon et al. (104)	359	6	46	3.1±0.3	164±22	22±7	±70
Bleeker et al. (105)	173	6	56	3.1±0.3	173±27	21±7	80
Boriani et al. (106)	121	6	63	3.1±0.3	175±22	24±6	69
Bleeker et al.(107)	144	/6	53	3.1±0.4	157±26	21±8	70
Ypenburg et al. (108)	191	6	56	2.9±0.5	163±30	21±7	76
Pires et al. (109)	537	6	62	3.1±0.3	168±19*	22±7*	62
Yeim et al. (110)	100	6	46	3.1±0.2	158±28	27±6	71
Lellouche et al. (111)	164	6	47	3.2±0.4	158±37	22±7	65

LVEF: left ventricular ejection fraction; NYHA: New York Heart Association
* approximation (patients were divided into 4 groups)

Table 1B. Echocardiographic response rates (expressed as reduction in LVESV) in 15 currently largest observational CRT studies

Authors	No. of patients	Follow-up (mo)	Ischemic etiology (%)	NYHA class	QRS duration (ms)	LVEF (%)	Response rate (%)
Yu et al. (35)	54	3	41	3.2±0.4	147±25/155±33*	25±10	57 A
Yu et al. (112)	141	3/6	48	3.1±0.5	NA	27±7/24±11*	62 B
Notabartolo et al. (37)	49	3	69	3.1±0.5	158±31	24±9	59 A
Yu et al. (113)	56	3	50	3.2±0.4	NA	26±9	54 A
Murphy et al. (114)	54	6	54	3.0±0.3	157±34	27±8	44 A
Bleeker et al. (107)	144	3/6	53	3.1±0.4	157±26	21±8	56 A
Yu et al. (34)	55	3	51	3.2±0.4	NA	26±9	53 A
Jansen et al. (115)	69	3	55	3.1±0.3	172±30	21±7	55 A
Yu et al. (116)	76	3	49	3.0±0.2	NA	28±10	55 A
Zhang et al. (53)	50	3	48	3.2±0.4	151±27	27±9	60 B
Jansen et al. (117)	57	3	53	3.1±0.2	169±28	22±7	65 B
Fung et al. (118)	60	3	47	3.2±0.3	150±27/155±24*	23±8/23±7*	52 B
Yu et al. (119)	107	3	NA	3.2±0.5	NA	27±8	58 B
Fung et al. (120)	85	3	47	3.2±0.7	NA	27±9	52 B
Yu et al. (36)	265	3/10	56	3.1±0.4	NA	24±8	55 A

Abreviations as in Table 1A; ESV: end-systolic volume. * responders / non-responders
A reduction >15% in LVESV, B reduction >10% in LVESV

THE VALUE OF QRS FOR RESPONSE TO CRT

Initially, interventricular dyssynchrony (as reflected by QRS duration) was considered the most important mechanism underlying response to CRT. However, careful analysis of the individual CRT patients showed, that despite prolonged QRS duration, 30% of the patients showed no response to CRT (1,3). Accordingly, the value of the wide QRS complex has become questionable as a selection criterium. Kashani et al evaluated the value of baseline QRS duration by analyzing 34 CRT studies including 2063 patients (11). The authors demonstrated that despite a significant reduction in QRS after CRT initiation in 32 studies, a difference in baseline QRS duration between clinical responders and non-responders to CRT was only reported in 1 study (190±30 ms vs. 171±21 ms, p<0.01) (12). Mollema et al recently specifically addressed the value of baseline QRS duration for prediction of long-term clinical (improvement in NYHA class) and echocardiographic (reduction >10% in LV end-systolic volume, LVESV) CRT response in 242 patients (13). No differences in baseline QRS duration were noted between clinical responders and non-responders (165±21 ms vs. 164±25 ms, NS) as well as echocardiographic responders and non-responders (167±22 ms vs. 162±22 ms, NS). Importantly, baseline QRS duration showed no predictive value for both clinical and echocardiographic response (see Figure 1).

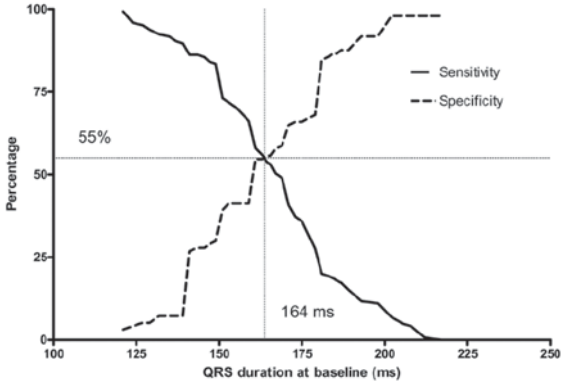

Figure 1. Value of QRS duration to predict response to CRT

Receiver-operating characteristic curve analysis for prediction of echocardiographic response. A cut-off value of 164 ms for QRS duration yielded a sensitivity and specificity of 55% to predict echocardiographic response. Adapted from Mollema et al (13).

Of note, pure LV pacing or sequential pacing with LV pre-excitation are associated with significant QRS prolongation, in stead of QRS shortening as demonstrated by CRT, and show nonetheless significant clinical benefit (14).

This failure of QRS duration to predict response may be explained by the fact that QRS duration mainly reflects interventricular dyssynchrony, whereas data suggest that LV dyssynchrony is more important for prediction of CRT response. Indeed, various studies demonstrated that QRS duration is mainly related to interventricular dyssynchrony, and does not reflect LV dyssynchrony (Figure 2) (15,16). Still, up to 70% of patients with wide QRS complex also have evidence of LV dyssynchrony on echocardiography, indicating that the likelihood of LV dyssynchrony is high in patients with wide QRS complex. Alternatively, the majority of patients with a QRS duration <120 ms does not have LV dyssynchrony on echocardiography (15-18).

To further explore the relative merits of interventricular and LV dyssynchrony for response to CRT, 24 echocardiographic studies on prediction of CRT response were evaluated. The results showed that only 2 studies provided some value of interventricular dyssynchrony for prediction

Figure 2. Relation between electrical and mechanical dyssynchrony

A. QRS duration correlates well with dyssynchrony between the left and right ventricle or interventricular dyssynchrony (IVMD, measured as the time difference between aortic and pulmonary pre-ejection intervals as determined with pulsed-wave TDI) Adapted from Ghio et al who evaluated 158 HF patients with LV ejection fraction <35% (13). B. There is no relationship present between LV dyssynchrony (measured as septal-to-lateral delay using color-coded TDI) and QRS duration. Adapted from Bleeker et al who evaluated 90 HF patients with LVEF <35% (15).

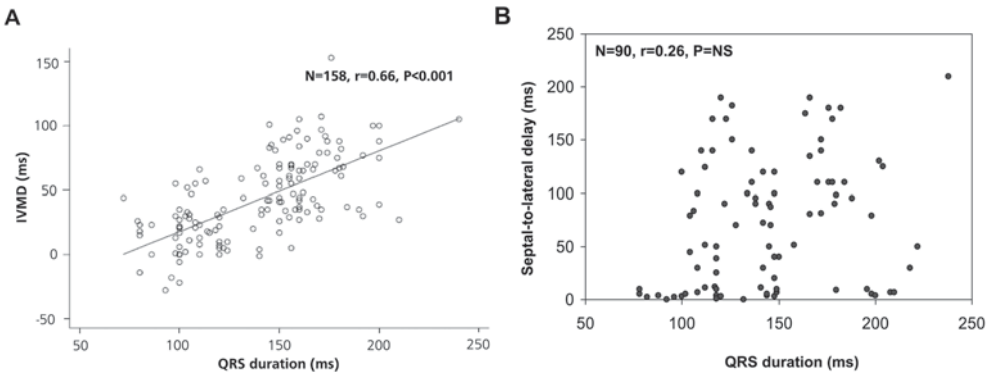

of CRT response, whereas all 24 studies demonstrated the value of LV dyssynchrony as a predictor of response (19).

Table 2. Echocardiographic studies on prediction of response to CRT

Author	Nr pts	F-up (mo)	Measurement	Description
Pitzalis et al. (21)	20	1	SPWMD	Septal-to-posterior wall motion delay
Pitzalis et al. (121)	60	6	SPWMD	Septal-to-posterior wall motion delay
Marcus et al. (22)	79	6	SPWMD	Septal-to-posterior wall motion delay
Bleeker et al. (23)	98	6	SPWMD	Septal-to-posterior wall motion delay
			Septal-to-lateral delay	Delay in Ts between basal septal and lateral wall
Diaz-Infante et al. (122)	67	6	SPWMD	Septal-to-posterior wall motion delay
Achilli et al. (26)	133	6	IVMD	Interventricular mechanical delay
Penicka et al. (12)	49	6	Sum asynchrony	Delay in Ts of 3 basal LV (septal, lateral, posterior) and basal RV segment
Yu et al. (33)	30	3	Ts-SD	SD of Ts of 12 LV segments
Bax et al. (30)	25	Acute	Septal-to-lateral delay	Delay in Ts between the basal septal and lateral wall
Bax et al. (31)	85	12	Septal-to-lateral delay	Delay in Ts between the basal septal, lateral, inferior and anterior wall
Notabartolo et al. (37)	49	3	PVD	Peak velocity difference; Max delay in Ts of 6 basal LV segments
Yu et al. (35)	54	3	Ts-SD	SD of Ts of 12 LV segments
Yu et al. (34)	55	3	SD-12	SD of Ts of 12 LV segments
			Diff-12	Max delay in Ts of 12 LV segments

ECHOCARDIOGRAPHY TO ASSESS CARDIAC DYSSYNCHRONY

Echocardiographic techniques provide the most practical approach to evaluate LV dyssynchrony and predict CRT response. These techniques include M-mode and Doppler echocardiography as well as tissue Doppler imaging (TDI) with post-processing imaging techniques such as strain, strain rate, tissue tracking, 2-dimensional (2D)-derived strain analysis, velocity vector imaging (VVI) and 3D echocardiography. Table 2 summarizes the echocardiographic studies on prediction of CRT response including the predictive values of the various parameters and techniques. Table 3 includes the advantages and limitations of each of the echocardiographic modalities. The results from the PROSPECT (Predictors of Response to Cardiac Resynchronization Therapy) trial demonstrated that most echocardiographic techniques have limited interobserver reproducibility, and significant training is required (20).

A. M-mode echocardiography

M-mode echocardiography is a relatively simple technique to assess LV dyssynchrony. Using the parasternal short-axis view of the LV at the level of the papillary muscles, the time interval between peak systolic contraction of the septum and the peak inward contraction of the posterior wall can be obtained, the so-called septal-to-posterior wall motion delay (SPWMD, Figure 3A). Pitzalis et al evaluated 20 HF patients with non-ischemic etiology, LVEF ≤35% and QRS ≥140 ms (21). A SPWMD of ≥130 ms appeared to be predictive for a reduction of ≥15% in LVESV after 1 month of CRT (21). Retrospective analysis of 79 patients from the CONTAK-CD

Technique	Definition of response	Cut-off value	Sens (%)	Spec (%)
M-mode	↓ ≥15% LVESV	≥130 ms	100	63
M-mode	↑ ≥5% LVEF	≥130 ms	92	78
M-mode	↓ ≥15% LVESV	≥130 ms	24	66
M-mode	↓ >10% LVESV	≥130 ms	65	48
		≥148ms	55	55
Color-coded TDI		≥65 ms	90	82
M-mode	↓ ≥15% LVESV	≥130 ms	50	38
Doppler	↑ ≥5% LVEF	>44 ms	66	55
Pulsed-wave TDI	↑ ≥25% LVEF	>102 ms	96	77
Color-coded TDI	↓ >15% LVESV	≥32.6 ms	100	100
Color-coded TDI	↑ ≥5% LVEF	≥60 ms	76	78
Color-coded TDI	↓ ≥15% LVESV	≥65 ms	92	92
Color-coded TDI	↓ ≥15% LVESV	≥110 ms	97	55
Color-coded TDI	↓ >15% LVESV	≥31.4 ms	96	78
Color-coded TDI	↓ >15% LVESV	≥31.4 ms	96	78
		≥98.5 ms	90	76

Table 2. Echocardiographic studies on prediction of response to CRT (continued)

Author	Nr pts	F-up (mo)	Measurement	Description
Knebel et al. (38)	38	6	Max delay	Max delay in Ts of 6 basal opposing walls
Yu et al. (36)	256	6 ± 3	Ts-SD	SD of Ts of 12 LV segments
			Ts-diff	Max delay in Ts of 12 LV segments
			TS-OW	Max delay in Ts of opposing walls of 12 LV segments
				Delay in Ts between basal septal and lateral wall
			Ts-sept-lat	
Van de Veire et al. (123)	49	Acute	Ts-SD-6	SD of Ts of 6 basal segments
			Ts-SD-12	SD of Ts of 12 LV segments
			Max delay-6	Max delay in Ts of 6 basal segments
			Max delay-12	Max delay in Ts of 12 LV segments
			Septal-to-lateral delay	Delay in Ts between basal septal and lateral wall
Van de Veire et al. (39)	60	6	Ts-SD-12	SD of Ts of 12 LV segments
Gorcsan et al. (124)	29	Acute	(Antero)septal-to-posterior delay	Max delay in Ts between (antero)septal and posterior wall
Yu et al. (113)	56	3	Ts-SD	SD of Ts for 12 LV segments in ejection phase
Van de Veire et al. (40)	60	6	LV dyssynchrony	Delay in Ts between basal septal and lateral wall
Tada et al. (56)	22	27±9	IVCDmax	Max LV intraventricular conduction delay = Delay in Ts between basal septum and lateral wall
Dohi et al. (43)	38	Acute	Radial dyssynchrony	Delay in Tε between basal septum and posterior wall
Porciani et al. (57)	59	6	o-ExCT	Sum of time exceeding aortic closure of 12 LV segments
				SD of Ts in 12 LV segments
			Ts-SD-12	
Suffoletto et al.(47)	64	8	Radial dyssynchrony	Delay in Tε between anteroseptal and posterior wall
				Max delay in Ts of 12 LV segments
			Ts-diff	SD of Ts of 12 LV segments
			Ts-SD	
Gorcsan et al. (49)	190	6 ± 3	Combined longitudinal	Delay in Ts between basal septal and lateral wall
			and radial dyssynchrony	Delay in Tε between anteroseptal and posterior wall
Delgado et al. (50)	161	6	AS-P delay	Delay in Tε between anteroseptal and posterior wall

Technique	Definition of response	Cut-off value	Sens (%)	Spec (%)
Color-coded TDI	↓ ≥15% LVESV + ↑ ≥5% LVEF	≥105 ms	64	80
Color-coded TDI	↓ >15% LVESV	≥33ms	93	78
		≥100 ms	92	68
		≥90 ms	81	80
		≥60 ms	70	76
Tri-plane TDI	↓ ≥15% LVESV	≥36.5 ms	91	81
		≥35.8 ms	91	85
		≥95 ms	74	81
		≥95 ms	74	81
Color-coded TDI		≥65 ms	87	81
Tri-plane TDI	↓ ≥15% LVESV	>33 ms	90	83
TSI	↑ ≥15% stroke volume	≥65 ms	87	100
TSI	↓ ≥15% LVESV	>34 ms	87	81
TSI	↓ ≥15% LVESV	≥65 ms	81	89
TSI	↓ ≥15% LVESV	>150 ms	100	90
TDI-derived strain (radial)	↑ ≥15% stroke volume	>130 ms	95	88
TDI-derived strain (longitudinal)	↓ ≥15% LVESV	≥760 ms	94	83
Color-coded TDI				
		≥32 ms	82	39
2D-Strain (radial)	↑ ≥15% LVEF	≥130 ms	89	83
Color-coded TDI		≥65 ms	89	75
		≥34 ms	89	75
Color-coded TDI	↑ ≥15% LVEF	≥60 ms		
2D-strain (radial)		≥130 ms	88	80
2D-strain (radial)	↓ ≥15% LVESV	≥130 ms	83	80

Table 2. Echocardiographic studies on prediction of response to CRT (continued)

Author	Nr pts	F-up (mo)	Measurement	Description
Yu et al.(34)	55	3	SD-12	SD of Td of 12 LV segments
			Diff-12	Max delay in Td of 12 LV segments
Cannesson et al. (51)	23	8	Dyssynchrony	Max delay in Ts of opposing walls of 6 LV segments
Ajmone Marsan et al. (54)	60	Acute	SDI	Systolic dyssynchrony index = SD of Tv for 16 LV segments

EF: ejection fraction; ESV: end-systolic volume; LV: left ventricular; RT3DE: real-time 3-dimensional echocardiography; SD: standard deviation; Td: time from onset of QRS to peak displacement; Tε: time from onset of QRS to peak systolic strain; Ts: time from onset of QRS to peak systolic velocity; Tv: Time from onset of QRS to minimum systolic volume; TDI: tissue Doppler imaging; TSI: tissue synchronization imaging; TT: tissue tracking; VVI: velocity vector imaging.

trial revealed less favorable results (22). SPWMD measurement yielded only limited predictive value for CRT response (sensitivity 24%, specificity 66%, Table 2). More importantly, in 45% of the study population the SPWMD measurement could not be obtained (Figure 3B, Table 3). Recent data in 98 patients also reported poor feasibility of M-mode imaging to assess LV dyssynchrony, due to the absence of a clear systolic deflection on M-mode echocardiography (53% akinesia of the septum, 12% akinesia of the posterior wall, or 3% both) or a poor acoustic window in the parasternal view (32%) (23). Therefore, M-mode has limited value in patients with scar formation in the antero-septal and posterior walls.

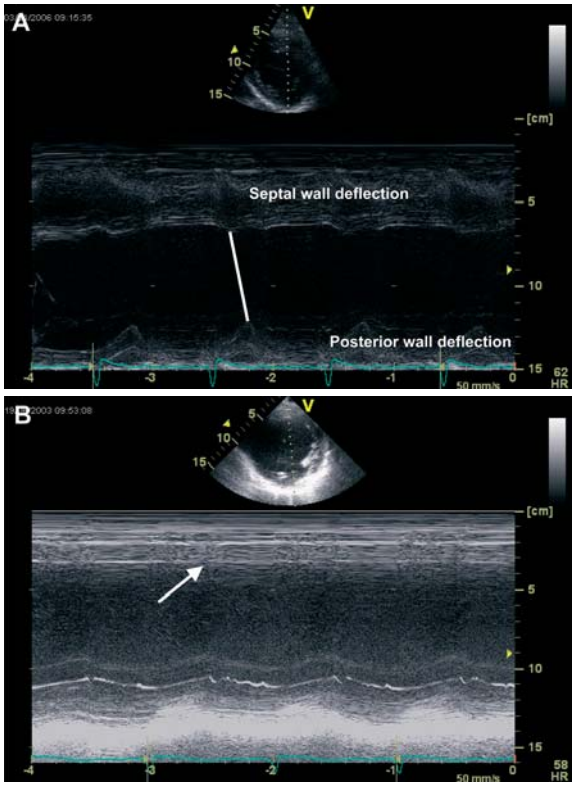

Figure 3. M-mode echocardiography

A. Parasternal M-mode recording of the LV in a HF patient. A clear delay between peak systolic septal and posterior wall inward motion can be seen (white line). B. Parasternal M-mode recording of the LV in a HF patient. Assessment of septal-to-posterior wall motion delay (SPWMD) is not possible due to the presence of an akinetic septum (arrow).

Technique	Definition of response	Cut-off value	Sens (%)	Spec (%)
TT	↓ ≥15% LVESV	≥75 ms	66	73
		≥205 ms	62	62
VVI	↑ ≥15% LVEF	≥75 ms	85	80
RT3DE	↓ ≥15% LVESV	≥5.6%	88	86

B. Doppler echocardiography

Doppler echocardiography can document dyssynchrony at various levels. AV dyssynchrony can be assessed by determining the LV filling time (LVFT) corrected for variations in heart rate (R-R interval). A LVFT/RR of <40% indicates AV dyssynchrony (24).

The LV-pre-ejection interval (LPEI) is defined as the time between the beginning of ventricular activation (QRS complex) and the beginning of LV ejection (onset aortic flow by Doppler echocardiography). A delay of ≥140 ms represents interventricular delay. Interventricular mechanical delay (IVMD) can also be assessed by measuring the pre-ejection intervals from the onset of QRS to the onset of aortic valve closure and pulmonic valve closure, respectively.

Figure 4. Doppler Interventricular mechanical delay (IVMD)

To measure IVMD, time to onset of flow is measured in the RVOT (A) and LVOT (B). Normal flow delays do not exceed 40 ms (A and B). C and D illustrate a dyssynchronous heart with a delay of 100 ms between RVOT flow (C) and LVOT flow (D).

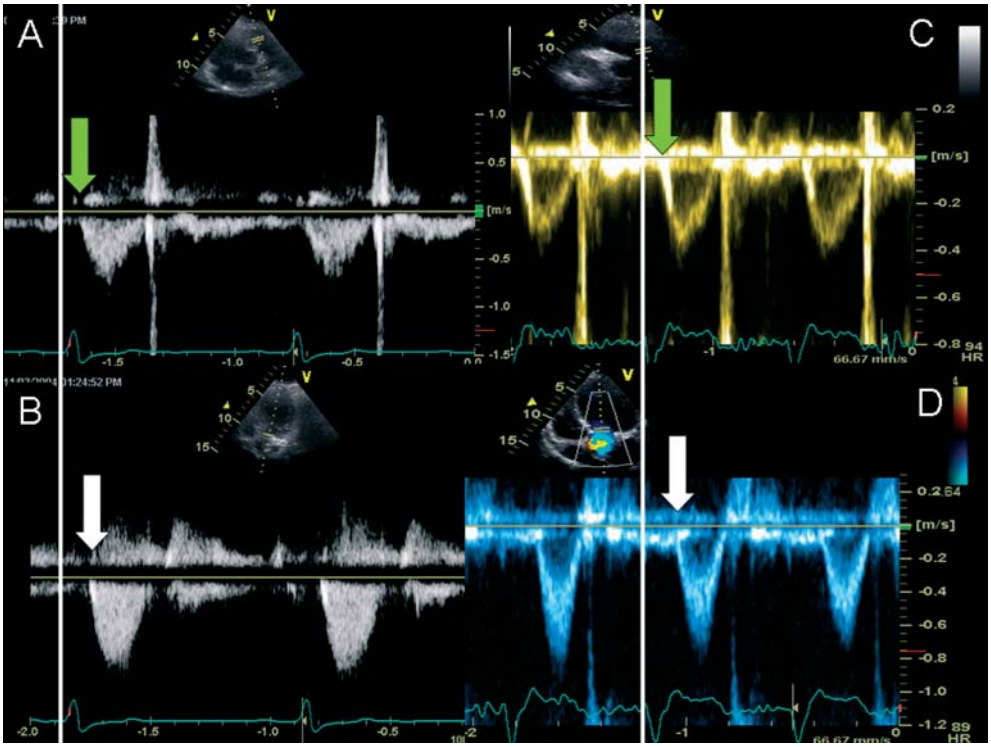

The IVMD is calculated as the difference between these 2 measurements and should be <40 ms (Figure 4) (6,24).

Delayed activation of the lateral wall (LLWC) is calculated as the percentage of overlap between the end of lateral wall contraction on M-mode echocardiography and the onset of LV filling (onset of the E-wave on pulsed-wave Doppler of transmitral flow). Any overlap represents intraventricular dyssynchrony (24).

The protocol of the CARE-HF (Cardiac Resynchronization in Heart Failure) trial included LPEI, IVMD and LLWC measurements for cardiac dyssynchrony. At least 2 of the above criteria were required to confirm the presence of cardiac dyssynchrony in patients with QRS duration between 120 and 149 ms.

However, available evidence on the predictive value of these dyssynchrony parameters is still limited. Bordachar et al evaluated 41 HF patients and despite the significant reduction of IVMD after CRT initiation (from 58±28 ms to 31±18 ms, p<0.001), no relation was found between IVMD and hemodynamic improvement acutely after CRT (25). Longer follow-up was obtained in the SCART (Selection of Candidates for CRT) trial which reported significantly longer IVMD's in responders as compared to non-responders (52±26 ms vs. 36±44 ms, p=0.029) (26). Furthermore, a IVMD >44 ms was able to predict combined clinical and echocardiographic response after 6 months of CRT with a sensitivity of 66% and a specificity of 55% (Table 2), whereas LLWC and pulsed-wave TDI parameters showed no predictive value. In addition, recent sub-analysis of the CARE-HF trial demonstrated that IVMD >49 ms together with low systolic blood pressure (<117 mmHg) was predictive for hospitalization-free survival after CRT (27).

C. Tissue Doppler imaging

TDI is one of the most popular techniques for the evaluation of LV dyssynchrony. TDI includes assessment of myocardial velocity in different myocardial regions and relating the timing of myocardial velocity to electrical activity (QRS complex), providing electro-mechanical delays. Data can be acquired on-line using pulsed-wave TDI or reconstructed off-line using color-coded TDI.

1. Pulsed-wave TDI

Initially, pulsed-wave TDI was used to assess cardiac dyssynchrony. A sample can be placed in the region of interest using 2D TDI images. This allows for quick online evaluation of regional synchronicity by measuring the time to onset of mechanical contraction in the ejection phase (Figure 5). This approach has shown a relationship between improvement in cardiac function after CRT and baseline LV dyssynchrony (28,29). Penicka et al measured time intervals in the 4 basal LV segments and in the basal segment of the free wall of the right ventricle (12). The authors reported a cut-off value of >102 ms for dyssynchrony (defined as the sum of LV and interventricular delay) for the prediction of improved LV function after CRT, yielding a sensitivity of 96% and a specificity of 77% (Table 2).

The restricted assessment of only one sample area at a time constitutes a major disadvantage of this method, whereas color-coded TDI permits simultaneous examination of multiple myocardial segments, thereby avoiding potential errors from differences in cardiac frequency. Furthermore, the timing of the LV ejection phase is very difficult to superimpose on the pulsed-TDI spectral Doppler waveform, which is another limitation (Table 3).

Table 3. Advantages and limitations of the main echocardiographic techniques for assessment of LV dyssynchrony for prediction of response to CRT

Technique	Advantages	Limitations
M-mode	Widely available Rapid assessment	Low feasibility / reproducibility in patients with ischemic cardiomyopathy and extensive scar tissue
Pulsed-wave TDI	Widely available	Difficult acquisition / time-consuming Susceptible to influences of breathing, patient motion and changes in heart rate Off-line analysis not possible Angle-dependent Cannot differentiate passive motion from active deformation
Color-coded TDI	Off-line rapid analysis	Requires specialized equipment High image quality needed Angle-dependent Cannot differentiate passive motion from active deformation
TSI	Rapid analysis Complete analysis of all LV segments Attractive Visual presentation	Requires specialized equipment High image quality needed Angle-dependent Cannot differentiate passive motion from active deformation
TDI-strain	Can differentiate passive motion from active deformation	Requires specialized equipment Significant operator experience needed Time-consuming Angle-dependent
2D-strain	Automated tracking algorithm Can differentiate passive motion from active deformation No angle-dependency	Requires specialized equipment Significant operator experience needed Time-consuming
VVI	Automated tracking algorithm Can differentiate passive motion from active deformation No angle-dependency	Requires specialized equipment Significant operator experience needed Time-consuming
RT3DE	Complete analysis of all LV segments	Requires specialized equipment Significant operator experience needed Time-consuming Lower spatial and temporal resolution

Abbreviations as in Table 2.

2. Color-coded TDI

A major advantage of color-coded TDI is the ability of off-line analysis. Importantly, the size and the positioning of the samples (region of interest) can be adjusted manually within the LV wall to identify where the peak systolic velocity is most reproducible.

In the early color-coded TDI studies of LV dyssynchrony, sample volumes were placed in the basal septal and lateral segments (apical 4-chamber view). By measuring the time to peak systolic velocity of the individual segments with reference to the QRS complex, the time difference between 2 segments was calculated (Figure 6). A "septal-to-lateral delay" of ≥60 ms appeared to be predictive of an immediate response after CRT (30). Subsequently, a 4-segment model was proposed including 4 basal segments (septal, lateral, inferior, and anterior) and a delay

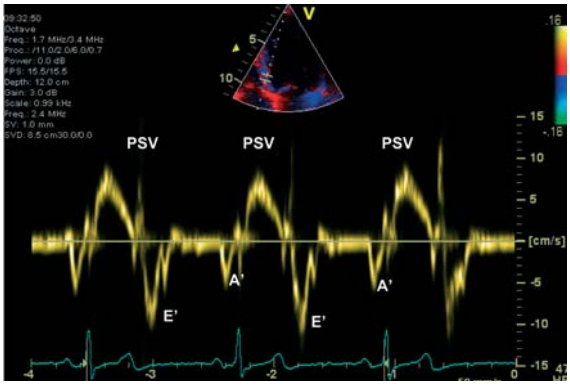

Figure 5. Pulsed-wave tissue Doppler imaging of a normal individual

The pulsed-wave sample is placed on-line in the region of interest and the myocardial velocity curve is derived. (PSV = peak systolic velocity, E' and A' are early and late diastolic velocities).

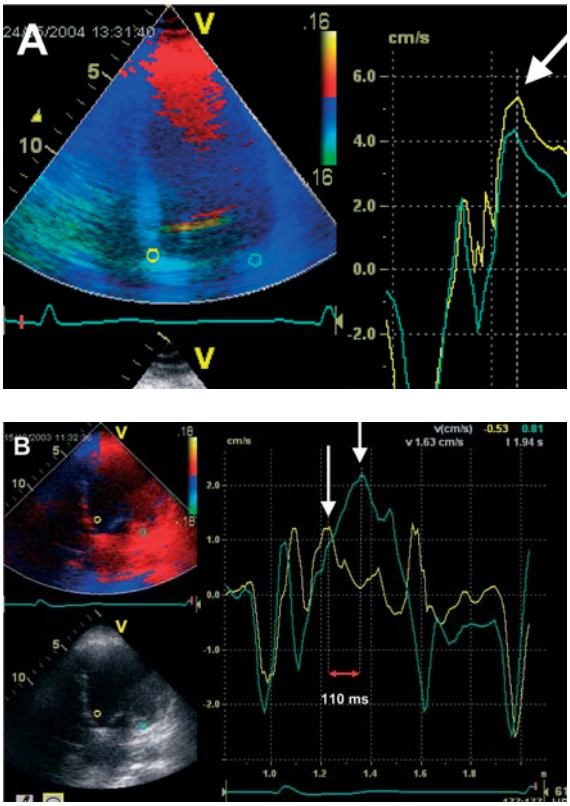

Figure 6. Color-coded tissue Doppler imaging

Color-coded 4-chamber TDI image in the upper left panel with off-line post-processing velocity tracings at the right side. A. Example of synchronous contraction without delay in peak systolic velocities. The peak systolic velocities of the septum (yellow) and the lateral wall (green), as indicated by the white arrow, occur at the same time. B. Example of severe LV dyssynchrony as indicated by the time delay in peak systolic velocity of the septum (arrow yellow curve) compared with the lateral wall (arrow green curve) of 110 ms.

of ≥65 ms was predictive of both clinical (sensitivity/specificity 80%) and echocardiographic improvement (sensitivity/specificity 92%) after 6 months of CRT (Table 2) (31).

Other studies used a "multi-segment model" to determine LV dyssynchrony to predict a favorable CRT response. A 12-segment model was proposed by Yu et al including 6 basal and 6 mid myocardial segments to assess LV dyssynchrony (32). The authors proposed to calculate a dyssynchrony index (Ts-SD) by using the standard deviation of all 12 time intervals. Initial work in 30 patients reported a Ts-SD of ≥32.6 ms to be predictive of LV reverse remodeling after CRT (33). The same group performed subsequent studies in larger patient groups comparing

multiple TDI-derived parameters, however, all studies showed best predictive value for Ts-SD-12 (see Table 2) (34-36). For instance, a recent study in 256 CRT patients showed that LV reverse remodeling after CRT (defined as a reduction of ≥15% in LVESV) could be predicted by 4 different TDI dyssynchrony parameters; a cut-off value of 33 ms for Ts-SD was able to predict response to CRT with a sensitivity of 93% and specificity of 78% (36).

Notabartolo et al measured the time to peak systolic velocity in the 6 basal segments (septal, lateral, anterior, inferior, anteroseptal and posterior) in 49 patients undergoing CRT (37). The peak velocity difference (PVD) was measured as the time difference between the earliest and latest contracting segment. A PVD of ≥110 ms at baseline was predictive of LV reverse remodeling at the 3-month follow-up (sensitivity 97%, specificity 55%). In addition, Knebel et al measured the maximal delay between the 6 opposing basal segments, and found a delay of ≥105 ms predictive for response to CRT (38).

Recently, it has become possible to acquire a tri-plane dataset (3D) and color-coded TDI of the LV simultaneously. The advantage of the tri-plane method is that acquisition of a single tri-plane dataset allows simultaneous comparison of 12 LV segments during the same heartbeat whereas the 2D method requires at least 3 acquisitions. During post-processing, this technique presents the timing of peak systolic velocities in a color-map in the apical 4-, 2-, and 3-chamber views. Furthermore, a 3D volume can be generated semi-automatically by tracing the endocardial

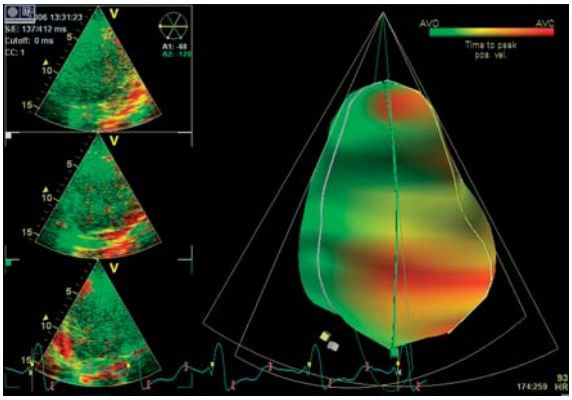

Figure 7. Tissue synchronization imaging

Using a tri-plane probe, color-coded tissue Doppler data from the apical 4-,2- and 3-chamber views are recorded simultaneously during the same heartbeat. During post-processing a 3D volume of the left ventricle is generated. The colors represent mechanical activation times. The orange-yellow color indicates later activation of the anterolateral wall compared to the septum (green).

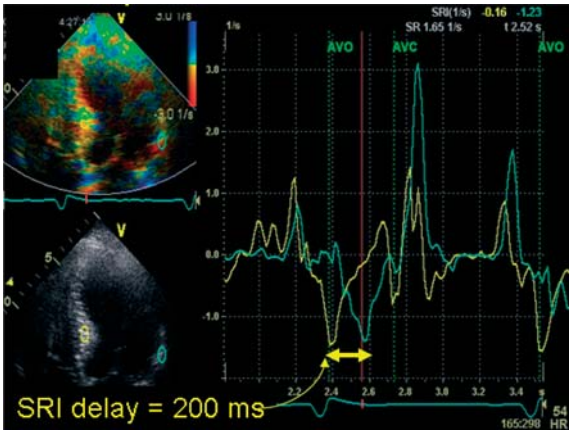

Figure 8. Strain rate imaging

Strain rate tracings obtained from the basal septum (yellow) and lateral wall (green) indicate a delay of 200 ms.

borders manually. Van de Veire and colleagues applied this technique in 60 patients and calculated dyssynchrony as the standard deviation of time to peak systolic velocity of the 12 LV segments (Ts-SD-12) (39). Patients showing LV reverse remodeling after 6 months of CRT had higher baseline values of Ts-SD-12 as compared to non-responders (42±14 ms vs. 22±12 ms, $p<0.05$). As a result, a cut-off value of ≥33 ms was able to predict response with a sensitivity of 90% and a specificity of 83% (Table 2). This cutoff value of 33 ms obtained with tri-plane TDI is similar to the cutoff value proposed by Yu et al when single-plane TDI was used (33).
Accordingly, a wide variety of TDI-based approaches has been developed recently to quantify LV dyssynchrony ranging from 2- to 12-segmental models (Table 2).

D. Tissue synchronization imaging

Tissue synchronization imaging (TSI) is another evolving technique. This technique can color-code the myocardium based on automated time-to-peak systolic longitudinal velocity of each segment. The resultant color-coded images permit a quick visualization of the earliest activated segments (displayed in green) and the latest activated segments (displayed in red) (Table 3). In addition, quantitative assessment is possible using myocardial velocity curves (similar to TDI). Van de Veire et al defined LV dyssynchrony as the time difference between basal septum and lateral wall, which was automatically calculated by the software (40). An excellent correlation was found between manually and automatically derived LV dyssynchrony ($r=0.95$, $p<0.0001$). In addition, TSI was able to predict LV reverse remodeling after 6 months of CRT (sensitivity 81%, specificity 89%, Table 2) using a cut-off value of 65 ms (similar to TDI).
More recently, TSI has been used in combination with tri-plane (3D) imaging, which permits for quick visualization of the most delayed LV segment (Figure 7). Nevertheless, long-term data using TSI are lacking and its superiority over standard 2D color-coded TDI has not been demonstrated.

E. TDI-derived strain (rate) imaging and tissue tracking

Strain imaging can be performed by off-line analysis of color-coded TDI images. In contrast to TDI, which only measures myocardial velocities, strain imaging is able to measure the percentage of myocardial deformation during systole using the Doppler velocity gradients (Figure 8). Negative strain values represent active contraction whereas positive values represent relaxation or lengthening, thereby differentiating active myocardial contraction from passive displacement. In addition, the rate of myocardial deformation, or strain rate, can be calculated. Strain imaging has been suggested to reflect myocardial dyssynchrony by measuring the time delays of time-to-peak systolic strain (comparable to TDI) (41,42). Initial studies applied strain imaging on the apical views, thereby measuring longitudinal strain, and reported low reproducibility due to the relatively high operator and angle dependency (41) (Table 3). Possibly related to these limitations, longitudinal strain appears a relatively poor predictor of CRT response as compared to TDI (34,35). Recently, Yu et al evaluated the value of TDI-derived longitudinal strain as compared to TDI in 256 CRT patients (36). The standard deviation of 12 LV segments of time to peak systolic velocity was significantly higher in responders as compared to non-responders (46±13 ms vs. 29±11 ms, $p<0.001$), whereas the standard deviation of 12 LV segment of time to peak myocardial strain was not different between responders and non-responders (65±31 ms vs. 67±28 ms, NS). Consequently, longitudinal strain was not able to predict response to CRT in this particular study.

Another study applied strain imaging on the short-axis views thereby measuring radial strain showing better results. Dyssynchrony was defined as the time difference of peak radial strain in the septum versus the posterior wall, and was significantly greater in patients with acute hemodynamic responses to CRT. Patients with dyssynchrony of ≥130 ms revealed an immediate improvement in stroke volume (sensitivity 95% and specificity 88%) (43).

Tissue tracking (TT) describes the systolic longitudinal motion or displacement and allows identification of delayed longitudinal contraction (DLC). To date, only few studies used this technique to quantify LV dyssynchrony. Yu et al evaluated 55 HF patients prior to implantation and calculated 6 different TT-derived measurements (34). A cut-off value of ≥75 ms for SD of time to peak displacement of 12 LV segments yielded a sensitivity of 66% and specificity of 73% to predict response (see Table 2). TT was also used by Sogaard et al who focused on the DLC during post-systole in order to assess LV dyssynchrony (44). LV dyssynchrony can be determined by calculating the number of myocardial segments with peak systolic excursion after aortic valve closure and by measuring the magnitude of the delay for each segment. In patients with ≤2 segments displaying DLC (n = 11) the acute improvement in LVEF after CRT initiation was significantly lower as compared to patients with >2 segments (n = 14) (10±7% vs. 32±15%, $p<0.01$). Also, subsequent studies by the same group with longer-term follow-up showed predictive value for the extent of myocardium showing DLC (45,46).

F. 2D derived strain imaging

A new echocardiographic technique, speckle tracking, can calculate myocardial strain from conventional 2D echocardiography. The main advantage of speckle tracking over TDI-derived strain is its lack of angle dependency (Figure 9, Table 3). Currently, only few studies involved this technique for assessment of LV dyssynchrony (38,47-50).

Suffoletto et al applied speckle tracking to routine mid ventricular 2D short-axis images in 48 patients undergoing CRT and time to peak radial strain was calculated from the 6 LV segments. Using a cut-off value of ≥130 ms for LV dyssynchrony (time difference in peak anteroseptal wall-to-posterior wall strain) yielded a sensitivity of 91% and a specificity of 75% to predict an immediate increase ≥15% in stroke volume. Long-term response (≥15% in LV ejection fraction) could be predicted with similar sensitivity and specificity (Table 2) (47). Importantly, speckle tracking analysis was possible in 96% of the patients with high reproducibility.

Recent work by Delgado et al evaluated all 3 forms of deformation using speckle tracking analysis including radial, circumferential and longitudinal strain in 161 HF patients undergoing CRT (50). Only radial strain was able to predict response to CRT; a cut-off value of 130 ms for the anteroseptal wall-to-posterior wall strain delay was able to predict LV reverse remodeling after 6 months of CRT (see Table 2).

G. Velocity vector imaging

VVI can also be applied to routine 2D images and allows measurement of myocardial velocity with an automated tracking algorithm. Cannesson et al applied this method to 23 CRT candidates. Tissue velocities were determined from standard apical 4-chamber, 2-chamber and long-axis views with high reproducibility. The greatest opposing wall peak longitudinal velocity delay from the 3 views indicates LV dyssynchrony. A baseline dyssynchrony of ≥75 ms predicted response to CRT (Table 2) (51).

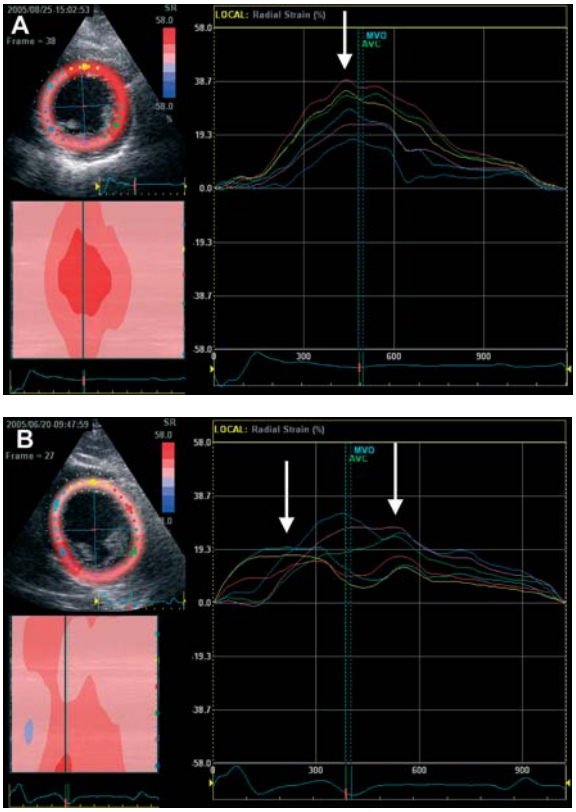

Figure 9. 2D-derived strain imaging or speckle tracking

A. Speckle tracking derived radial strain imaging in the parasternal short-axis view at the mid LV level. In this example peak radial strain (arrow) occurs simultaneously in all 6 segments, indicating a synchronous LV contraction (the curves are color-coded in accordance with the segments on the short-axis view). B. Example of radial time-strain curves from speckle tracking in a HF patient with LV dyssynchrony. The septal regions reach peak strain early in systole (blue/yellow curves), whereas the lateral segments reach peak strain late in systole (red/green curves, arrows indicate peak systolic strain).

Figure 10. Real-time 3D echocardiography

Example of LV dyssynchrony analysis from a RT3DE data set using parametric images. The global time from onset of QRS to mean systolic volume is used as timing reference; early segments are coded in blue, whereas late segments are coded in red. A. Before CRT, the postero-lateral segments are activated last (indicated in red). Substantial dyssynchrony is present as indicated by a systolic dyssynchrony index (SDI) of 9.7%. B. After 6 months of CRT the overall green color indicates absence of regions with delayed activation, indicating resynchronization after CRT implantation (SDI 1.1%).

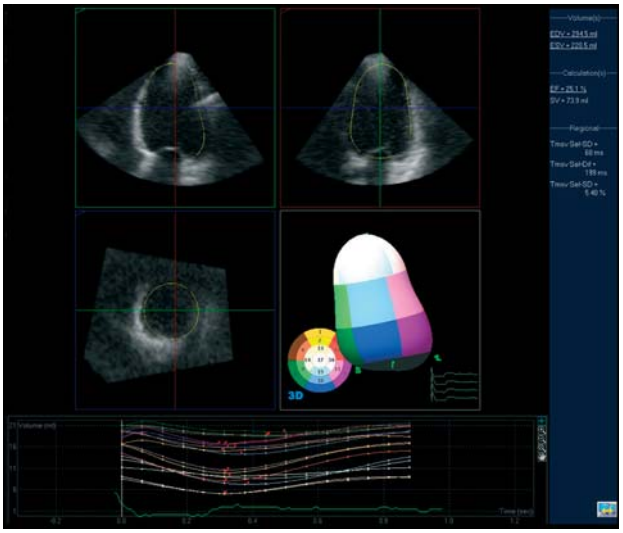

H. Real-time 3D echocardiography

Real-time 3D echocardiography (RT3DE) is another new technique which determines dyssynchrony in 16 LV segments by color-coding each segment and quantifying regional function and change in volumes for each segment during systole and diastole. The degree of dispersion in the timing of minimal volume for each segment reflects the extent of LV dyssynchrony (Figure 10). The systolic dyssynchrony index (SDI) is used as a marker for global LV dyssynchrony and is defined as the standard deviation of the timing for each segment. In addition, the area of latest activation can be identified.

This method can rapidly quantify LV dyssynchrony as demonstrated by Kapetanakis et al who evaluated 174 unselected patients referred for routine echocardiography (52). Also, Zhang et al evaluated 13 patients with RT3DE during a 15-min interruption of CRT and reported an increase of SDI, with an increase in LV volumes and a decrease in LVEF (53). Only 1 study currently addressed the predictive value of RT3DE for acute response after CRT (54); Ajmone et al found that a SDI of 5.6% was predictive for an immediate decrease in LVESV of ≥15% (sensitivity 88% and specificity 86%, Table 2). Currently, no data are available on the prediction of long-term CRT response using this technique. However, limitations include low frame rates of 20 to 30 frames/sec for image acquisition and the inability to differentiate between passive motion and active deformation.

As discussed, several echocardiographic methods have been proposed for the quantification of LV dyssynchrony in HF patients; e.g. TDI using differences in myocardial velocities, strain using differences in myocardial deformation and 3D-echocardiography using differences in volume changes within the LV. To date there is no consensus on which technique best predicts response to CRT. Furthermore, numerous definitions of LV dyssynchrony have been advanced with varying numbers of LV segments to be evaluated and different cutoff values. Importantly, a compromise is necessary between the optimal method for detection of LV dyssynchrony and the feasibility in daily practice (Table 3). Most performed studies are small, single center, non-randomized studies with short-term follow-up. Furthermore, interpretation is confounded by varying definitions of response to CRT and availability of direct comparisons is lacking. At present, only 11 studies compared 2 or more echo techniques for prediction of response; 2 studies compared M-mode with TDI (23,55), 1 study compared TSI with TT (56), 4 studies compared several TDI-derived strain imaging parameters with TDI (34-36,57) and another 4 studies compared 2D-derived strain imaging parameters with TDI (38,47,49).[45]. Interestingly, in these studies TDI emerged as best in predicting response to CRT despite varying numbers of LV segments included in the assessment of LV dyssynchrony. Of note, 3 recent studies that applied 2D radial strain imaging demonstrated promising results with comparable (or even higher) predictive values for anteroseptal wall-to-posterior wall strain delay as compared to TDI (Table 2).

Larger multi-center studies are needed to identify the most useful technique, with the optimal number of segments to evaluate and the optimal extent of LV dyssynchrony, to select patients with a high likelihood of CRT response. Thus far, one prospective, multi-center study has been reported. The PROSPECT trial compared various echocardiographic techniques to assess LV dyssynchrony and predict response to CRT (20). The results however demonstrated that all echocardiographic techniques had limited predictive value for response to CRT. Major limitations included the limited assessability of LV dyssynchrony from the various echo techniques, but

also the poor inter-observer agreement for assessment of LV dyssynchrony. In addition to these technical shortcomings, pathophysiological issues may also have influenced response to CRT, including the presence of extensive scar tissue, limited venous anatomy and suboptimal LV lead position, which will be discussed below.

THE VALUE OF MAGNETIC RESONANCE IMAGING

The use of MRI for selecting patients for CRT is increasing. Cardiac MRI can provide a detailed morphological and functional evaluation of the heart irrespective of the patient's anatomy

Table 3. Advantages and limitations of the main echocardiographic techniques for assessment of LV dyssynchrony for prediction of response to CRT

Technique	Advantages	Limitations
M-mode	Widely available Rapid assessment	Low feasibility / reproducibility in patients with ischemic cardiomyopathy and extensive scar tissue
Pulsed-wave TDI	Widely available	Difficult acquisition / time-consuming Susceptible to influences of breathing, patient motion and changes in heart rate Off-line analysis not possible Angle-dependent Cannot differentiate passive motion from active deformation
Color-coded TDI	Off-line rapid analysis	Requires specialized equipment High image quality needed Angle-dependent Cannot differentiate passive motion from active deformation
TSI	Rapid analysis Complete analysis of all LV segments Attractive Visual presentation	Requires specialized equipment High image quality needed Angle-dependent Cannot differentiate passive motion from active deformation
TDI-strain	Can differentiate passive motion from active deformation	Requires specialized equipment Significant operator experience needed Time-consuming Angle-dependent
2D-strain	Automated tracking algorithm Can differentiate passive motion from active deformation No angle-dependency	Requires specialized equipment Significant operator experience needed Time-consuming
VVI	Automated tracking algorithm Can differentiate passive motion from active deformation No angle-dependency	Requires specialized equipment Significant operator experience needed Time-consuming
RT3DE	Complete analysis of all LV segments	Requires specialized equipment Significant operator experience needed Time-consuming Lower spatial and temporal resolution

Abbreviations as in Table 2.

Figure 11. Tagged magnetic resonance imaging

MRI tissue tagging in a healthy volunteer. The tags appear as a grid superimposed on the short-axis view at the mid ventricular level. These taglines can be traced during the contraction (A end-diastolic, B end-systolic), enabling strain rate analysis on global and regional level during the cardiac cycle.

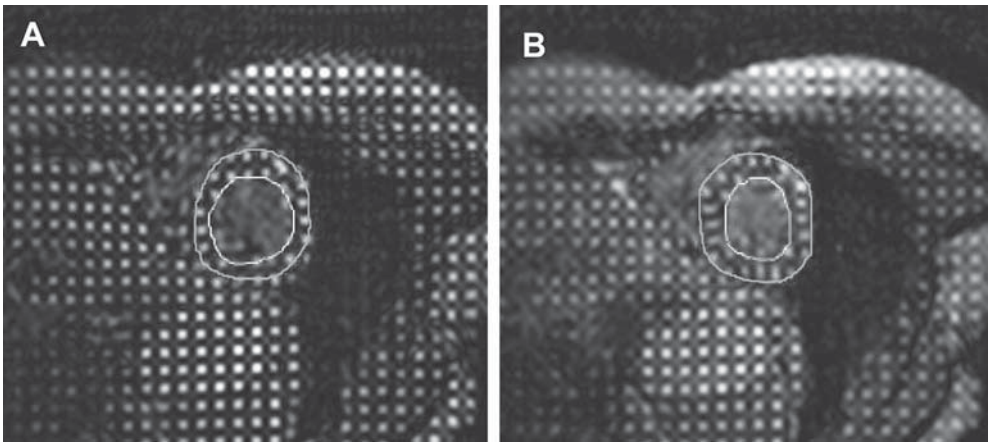

in any arbitrary orientation (58). Furthermore, MRI is particularly useful in patients with a suboptimal acoustic window. Both LV and interventricular delay in ventricular contraction patterns can be studied using 3 different applications of cardiac MRI.

A. Strain rate analysis from MRI tissue tagging

MRI tissue tagging labels the myocardium by selective saturation prepulses applied in a specific orientation perpendicular to the desired imaging plane. The tags appear as horizontal or vertical lines, or as a grid of both, superimposed on the image (4-chamber or short-axis view). These taglines can be traced during the contraction, enabling strain rate analysis on a global and regional level during the cardiac cycle. 3D MR tissue tagging has been used for studying LV dyssynchrony (59): in animal models with left bundle branch block-induced HF, an acute improvement in hemodynamic parameters as well as an acute improvement in intraventricular delay were noted after establishing mechanical synchrony by left atrial and biventricular pacing (60,61). In humans, the feasibility of assessing LV dyssynchrony with tagged MRI has been demonstrated in healthy volunteers (62) as well as in patients with ischemic and non-ischemic cardiomyopathy (63), but further testing is needed in CRT candidates (Figure 11). Still, this method is technically difficult which limits its routine use.

B. Velocity-encoded MRI

Phase-contrast velocity encoded MRI (64), when applied for myocardial wall motion measurement, allows evaluation of the myocardial velocity during contraction in any arbitrary orientation, such as the longitudinal, radial or circumferential contraction. Westenberg et al recently applied velocity-encoded MRI in HF patients with low LVEFs and wide QRS complexes, by measuring the longitudinal LV contraction and compared their results directly with TDI (65). The authors noted an excellent agreement between both modalities for classification according to the severity (minimal, intermediate or extensive dyssynchrony) of LV dyssynchrony (Figure 12). Similar results were demonstrated by Delfino et al, who reported excellent correlations for

Figure 12. Velocity-encoded magnetic resonance imaging

Velocity-encoded MRI and velocity graphs are presented in respectively the left and right panel, demonstrating extensive LV dyssynchrony with a septal-to-lateral delay of 116 ms. Adapted from Westenberg et al (65).

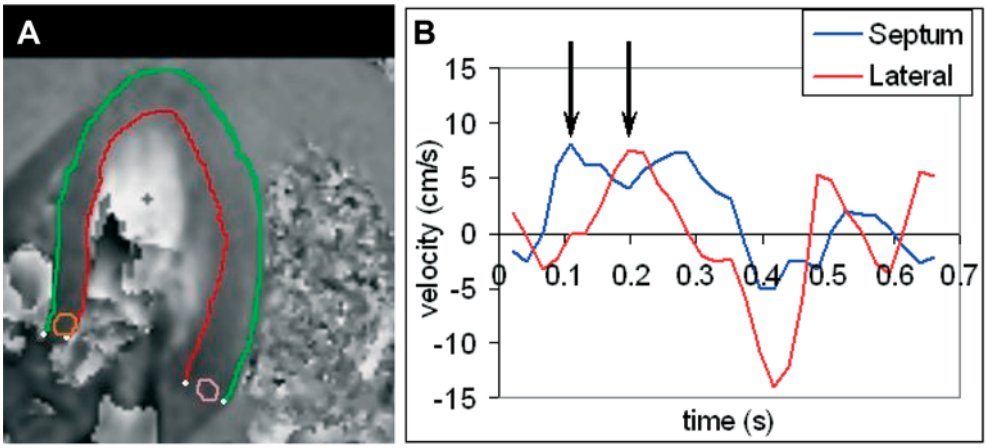

peak velocities (r=0.86) and time to peak velocities (r=0.97) as measured with TDI and MRI (66). Besides measuring the longitudinal myocardial wall velocities (basal-to-apex contraction and relaxation) in the 4-chamber orientation, MRI can also provide the radial, circumferential or longitudinal myocardial wall velocity acquired in a short-axis orientation (67). Regional analysis along the circumference of this short-axis, by measuring the time of peak systolic velocity, can indicate the site of latest activation.

C. Regional wall motion analysis from LV short-axis cine MRI

LV dyssynchrony can also be determined from regional wall motion analysis in 3 cine short-axis MRI slices. The standard 16-segment model is applied: 6 segments at basal level, 6 segments at mid ventricular level and 4 segments at apical level. In all phases, endocardial contours are determined at these 3 levels (68). Regional wall motion analysis for each of the 16 segments provides 16 individual graphs for wall motion. The standard deviation between the values of peak wall motion or peak wall thickness is an indicator of the extent of LV dyssynchrony (Figure 13).

Other information derived from MRI

Cardiac MRI is also of interest for evaluation of potential candidates for CRT, because other factors (apart from LV dyssynchrony) are important in patient selection. These factors include the size, shape and function of the LV (volumes, LVEF, sphericity) and the presence and transmurality of scar tissue at the site of LV lead placement. MRI can provide all this information with high accuracy due to high spatial and temporal resolution. With contrast-enhancement MRI, precise delineation of scar tissue is possible (69,70). Regions with scar tissue have large interstitial spaces between the collagen fibres, resulting in slower outwash of gadolinium-based contrast agent compared to regions of healthy myocardium. This is presented by an increased hyperenhancement on inversion-recovery MRI, as the T1 of the gadolinium-based

Figure 13. Wall motion analysis with magnetic resonance imaging

A. Regional wall motion analysis of short-axis MR slices at 3 different levels in a healthy volunteer. In all phases epicardial (red) and endocardial borders (green) are determined and a 16-segment model of de LV is applied: 6 segments at basal level, 6 segments at mid ventricular level and 4 segments at apical level. The standard deviation between the values of peak wall motion is an indicator of the amount of LV dyssynchrony. B. Example of complete synchrony in a healthy volunteer. C. Example of a patient with ischemic cardiomyopathy showing a differences in timing of peak wall motion (see arrows), indicating LV dyssynchrony.

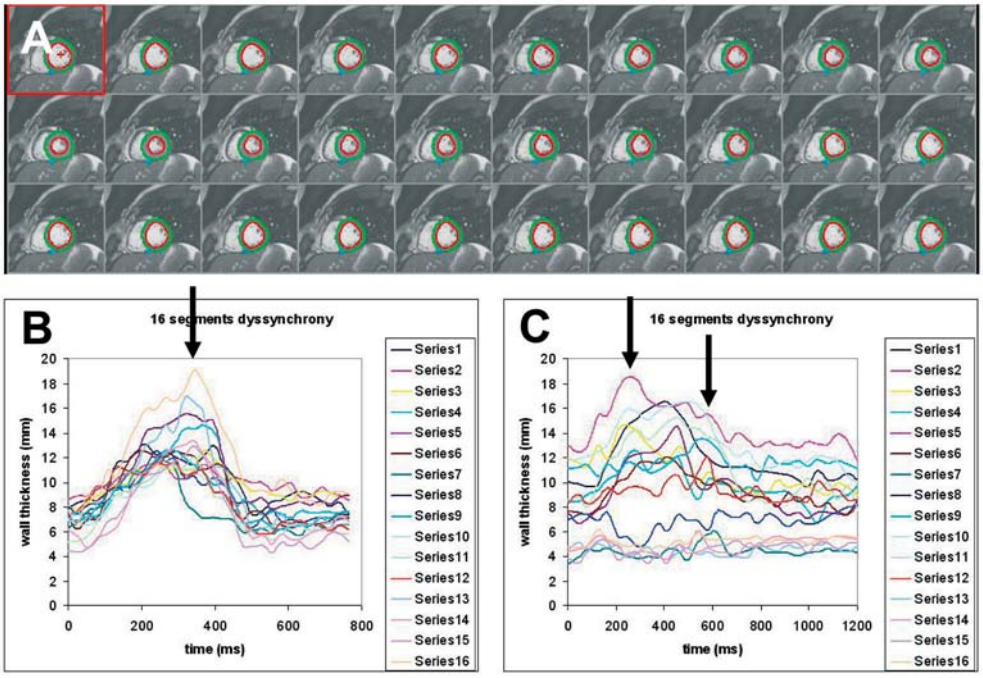

contrast is much shorter than that of myocardial tissue. Bleeker et al applied this technique and recently demonstrated that patients with transmural scar tissue in the posterolateral region (the preferred region for the LV pacing lead) do not respond to CRT despite the presence of baseline LV dyssynchrony (71) (Figure 14). In addition, not only the location of scar but also the extent of scar tissue ("scar burden") is important. Two studies addressed this issue and demonstrated that the more scar burden, the less improvement in LV function after CRT (72,73).

Lastly, recent small observations demonstrated feasibility of MRI to depict the coronary venous anatomy, which anatomic information can be used for LV lead positioning (74-76). However, a high spatial resolution of a 3D dataset is required to adequately depict the relatively small coronary vessels.

Thus, MRI is a method capable of simultaneously evaluating the presence of scar tissue, LV function, LV dyssynchrony and identifying a suitable vein for LV lead placement helping to better plan the CRT implantation strategy. However, the number of studies with long-term predictive value is limited.

In addition, cardiac MRI is not feasible in all patients; claustrophobia is occasionally a problem, and absolute contraindications include pacemakers (77), defibrillators, cerebral clips and

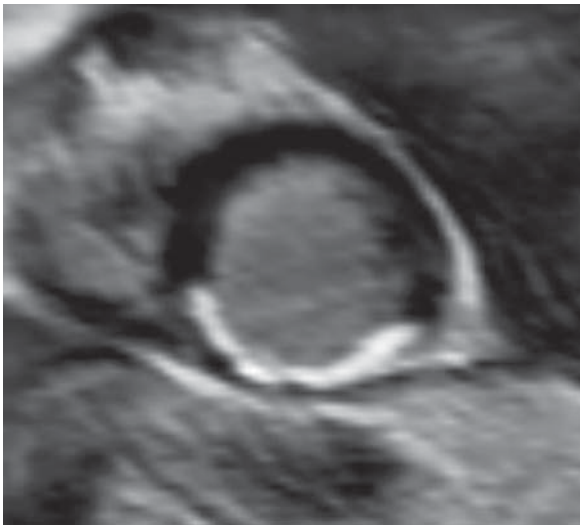

Figure 14. Contrast-enhanced magnetic resonance imaging

The presence and transmurality of scar tissue can be determined with contrast-enhanced MRI. This short-axis view demonstrates transmural scar (white area) in the postero-lateral region (preferred region of the LV pacing lead).

pregnancy. Some pacemakers and defibrillators, though, have shown MRI compatibility in experimental studies (78). Furthermore, relative precautions for contrast nephropathy should be made for patients with moderate to severe chronic kidney disease. Still, MRI is not suitable for follow-up of patients undergoing CRT. Another limitation of the MRI application in clinical routine is the time-consuming data acquisition and analysis. Image analysis software with automated segmentation algorithms are indispensable for handling large amounts of data acquired from cardiac MRI tests.

THE VALUE OF NUCLEAR IMAGING

A. Radionuclide angiography

Radionuclide angiography has been used mainly for the assessment of wall motion abnormalities and LVEF, but it can also be used for evaluation of cardiac dyssynchrony. Interventricular and LV dyssynchrony can be quantified using functional images, as assessed by Fourier analysis, with high reproducibility (79,80). Interventricular dyssynchrony is calculated as the difference between the mean phase angle of the LV and RV; LV dyssynchrony is calculated as the SD of the phase histogram. Only a few studies have used radionuclide angiography to assess LV dyssynchrony before CRT and the relationship to outcome after device implantation. One small study evaluated 13 patients and found a significant acute increase in LVEF and a significant decrease in interventricular and LV dyssynchrony during biventricular pacing, compared with normal sinus rhythm (81). Toussaint and colleagues used radionuclide angiography at baseline and 6 months after CRT implantation in 34 patients (82). The combination of a baseline LVEF >15% with interventricular delay was the best predictor of improvement in LVEF at 6 months follow-up. These results are not in line with those demonstrated with TDI (showing the greatest benefit of CRT in patients with LV rather than interventricular dyssynchrony), and further studies including comparisons with TDI are required.

B. SPECT

Recently, Chen and colleagues demonstrated in 90 normal individuals that gated SPECT imaging can also be used for the assessment of LV dyssynchrony (Figure 15) (83). These workers developed a count-based method to extract the amplitude and phase from regional LV count changes throughout the cardiac cycle. The phase information can be related to the time interval, and consequently the onset of mechanical contraction could be determined. Henneman et al correlated LV dyssynchrony as assessed with TDI with the parameters derived form gated SPECT (84). The authors analyzed 75 HF patients and demonstrated a good relationship between histogram bandwidth ($r=0.89$, $p<0.001$) and phase standard deviation ($r=0.80$, $p<0.001$). In a subsequent study the authors related both histogram bandwidth and phase standard deviation to response after 6 months of CRT (85). Cut-off values of 135° for histogram bandwidth and 43° for phase standard deviation were proposed to predict clinical response, defined as an improvement of ≥1 NYHA functional class after 6 months of CRT.

Other information derived from nuclear imaging

Similar to MRI, nuclear imaging is well-suited for assessment of viability and scar tissue. Sciagra et al demonstrated that patients were severe resting defects on ^{99m}Tc- sestamibi SPECT at baseline showed lack of response after CRT (86). Another study used ^{18}F-fluorodeoxyglucose SPECT to determine the extent of viable myocardium in 61 ischemic CRT candidates. The authors proposed a cut-off value of ≥11 viable segments (in a 17-segment model) to predict clinical response, yielding a sensitivity of 74% and a specificity of 87% (Figure 16) (87). Furthermore, scar tissue (defined as <50% tracer activity on ^{99m}Tc-tetrofosmin SPECT) in the region of the LV pacing lead prohibited both clinical and echocardiographic improvement after CRT (88). Similar results were demonstrated by Adelstein et al; higher overall scar burden, larger number of severely scarred segments, and greater scar density near the LV lead tip indicate an unfavorable response to CRT in ischemic patients (89).

THE VALUE OF COMPUTED TOMOGRAPHY

Studies on computed tomography (CT) in CRT candidates mainly focused on non-invasive visualization of the venous coronary anatomy. In clinical practice, retrograde invasive venography is used to determine venous anatomy during CRT implantation. Meisel et al evaluated the availability of veins for possible lead placement in 129 patients using CT. They reported that venous anatomy is highly variable and that not all patients are suited for endocardial (via the coronary sinus) LV lead placement (90).

Jongbloed et al demonstrated the feasibility of multislice CT (MSCT) for visualizing venous anatomy (Figure 17) (91). The same group recently demonstrated with 64-slice CT that patients with a history of extensive myocardial infarction were less likely to have a left marginal vein, which may hamper optimal LV lead positioning (Figure 18) (92).

A recent study by Aurrichio et al implemented the use of MSCT in 10 CRT recipients who presented with worsening HF symptoms (93). Besides visualization of the venous anatomy, the authors emphasized the importance of vein occlusion and proximity of the target vein to the

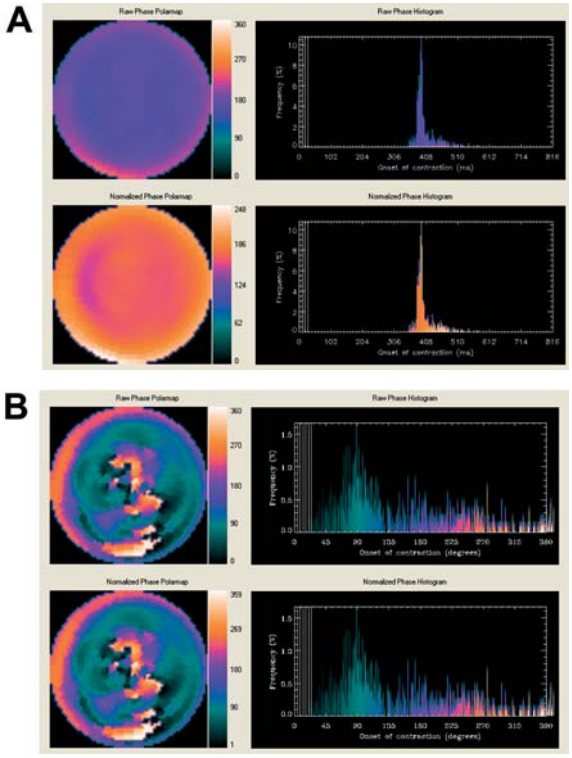

Figure 15. Phase analysis of ECG-gated myocardial perfusion SPECT imaging

A. Example of a synchronous contraction; the histogram shows a narrow and peaked distribution and the polar map is homogenous. B. Example of a dyssynchronous contraction; the histogram shows a wide distribution. The polar map indicates that the apex and posterior region of the myocardium show delayed contraction.

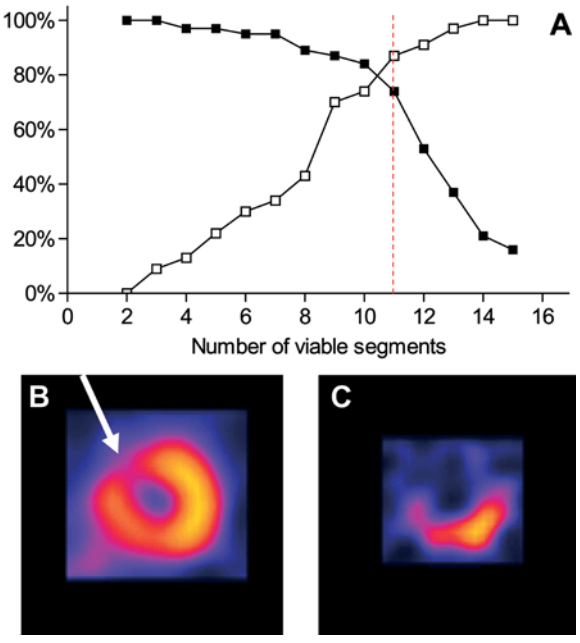

Figure 16. Viability assessment with FDG SPECT

A. Receiver-operating characteristic curve analysis on the extent of viability before CRT implantation and clinical response after 6 months of CRT, with the black line representing sensitivity and the white line representing specificity. The optimal cut-off value was identified at 11 viable segments, yielding a sensitivity of 74% and a specificity of 87%. Adapted from Ypenburg et al (87). B. Example of a responder to CRT with a small antero-septal scar (arrow) on FDG SPECT. C. Example of a non-responder with large scar formation on FDG SPECT with only few viable segments.

phrenic nerve or diaphragm to decide whether a transvenous or transthoracic approach may be preferred.

At present, MSCT is not routinely used to assess venous anatomy prior to CRT implantation. The main limitations include the radiation dose and the lack of information on the site of latest activation. Importantly, patient-related factors such as heart rate greater than 60 or 70 beats/min and irregular heart rhythm (atrial fibrillation or frequent atrial or ventricular extrasystoles), can interfere with the diagnostic quality of the images.

In addition, preliminary results in 21 patients showed promising results for assessment of LV function and myocardial perfusion when compared to nuclear imaging (94). Furthermore, assessment of cardiac dyssynchrony may be possible in the future with the new dual source CT due to the higher temporal resolution (95).

Figure 17. Venous anatomy using multi-slice computed tomography

Invasive venography (left panel) and 3D volume rendered reconstruction of a 64-slice CT acquisition (right panel) of the same patient with an idiopathic dilated cardiomyopathy. A large left marginal vein (LMV) is originating from the great cardiac vein (GCV).

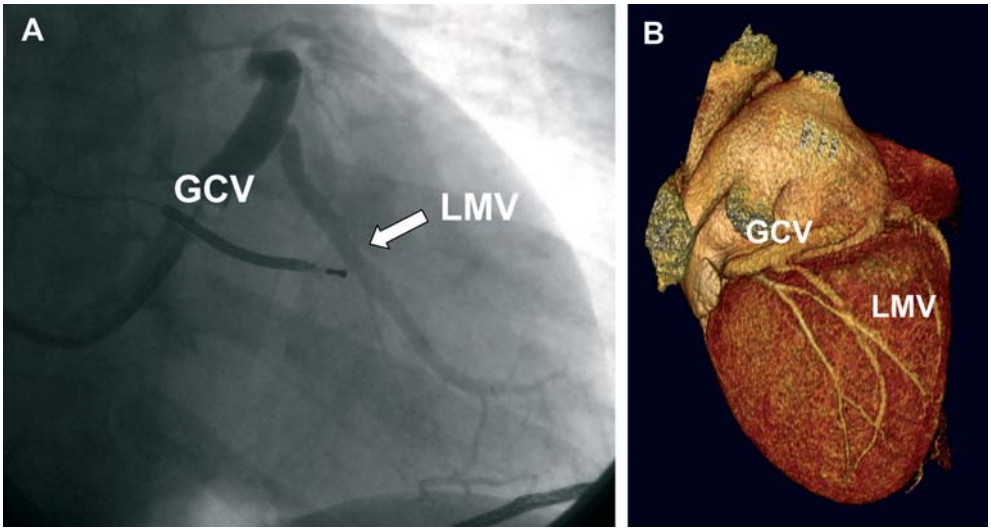

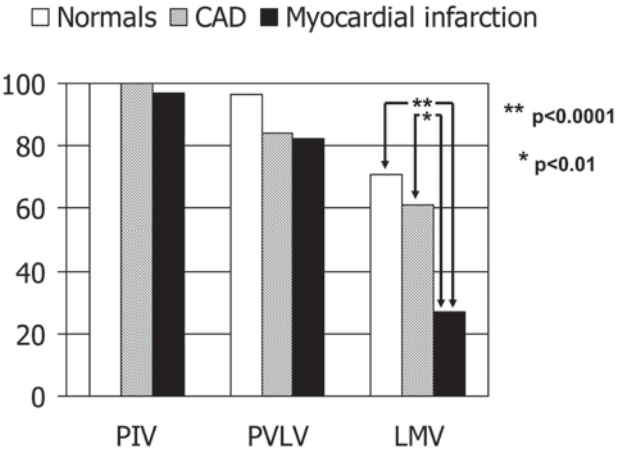

Figure 18. Venous anatomy

Prevalence – as assessed with 64-slice CT - of the posterior interventricular vein (PIV), posterior vein of the left ventricle (PVLV) and left marginal vein (LMV) in 28 normal controls, 38 patients with coronary artery disease (CAD) and 34 patients with a history of myocardial infarction. Patients with a history of myocardial infarction were less likely to have a LMV, as compared to normal controls. This may hamper left ventricular lead positioning in CRT. Adapted from Van de Veire et al (84).

BODY SURFACE POTENTIALS

Electrocardiographic imaging (ECGI) is a non-invasive cardiac electrical imaging modality that can image epicardial potentials, electrograms, and isochrones (activation sequences) using electrocardiographic measurements from body surface locations (96). Only one study applied this technique in 8 CRT candidates with LBBB using a 224-electrode vest to acquire body surface potentials at 1-millisecond intervals during the cardiac cycle (97). Electrical interventricular synchrony was quantified by the index Esyn, the mean activation time difference between the RV and LV free walls. The authors reported a wide range of electrical activation patterns with regions of delayed and/or absent conduction and development of functional lines of block. During CRT, mean Esyn improved from -76±24 to -31±-32 ms (P=0.01). Furthermore, some regions of slow conduction appeared in the LV in response to pacing, indicating functional electrical characteristics of local tissue. Still, improved Esyn did not consistently predict an improvement in LVEF during CRT, probably due to the fact that LV dyssynchrony is a better predictor than interventricular delay (19). Thus, patient-specific electrophysiologic substrate properties may determine outcome of CRT; however, its clinical role in CRT has yet to be determined.

CONCLUSIONS AND FUTURE PERSPECTIVES

Despite the impressive results of CRT in large randomized trials, 30-40% of the patients do not respond. In the search for more optimal selection criteria the presence of LV dyssynchrony at baseline appears important for clinical and echocardiographic improvement. To assess LV dyssynchrony, various non-invasive imaging techniques have been proposed. The most experience has been gathered with echocardiographic techniques, particularly color-coded TDI. Color-coded TDI has proven highly predictive for CRT response and event-free survival at 1-year follow-up in single-center studies. Other techniques including TSI, strain imaging, speckle tracking, 3D echocardiography need more investigation, but initial results are promising. Available evidence is limited on the value of non-echocardiographic imaging methods (particularly MRI and nuclear imaging) to assess LV dyssynchrony and prediction of CRT response. However, these techniques can provide other information, for instance the presence of scarred and viable myocardium and venous anatomy, potentially important for the selection of CRT candidates.

Although it is generally agreed that LV dyssynchrony is a major determinant of response to CRT, the recently published PROSPECT trial demonstrated only modest results of echocardiography to predict response to CRT (20). The major limitations, as outlined above, were non-assessability in a high percentage of patients, with low inter-observer agreement. On the other hand, the trial was also not ideal, since a substantial percentage of patients had LVEF >35%, without significant LV dilatation; in other words, these patients could not reverse remodel after CRT (which was one of the major endpoints in the trial). In addition, pathophysiological issues (scar tissue, venous anatomy, LV lead position) are important in the response to CRT and may need to be assessed before CRT implantation.

Accordingly, various questions may be addressed in patients considered for CRT. First, is substantial LV dyssynchrony present? Patient selection based on echocardiographic assessment showed a superior response rate compared to selection based on the current criteria, although larger studies are needed to define the best technology. Second, where is the area of latest activation for optimal positioning of the LV lead? As demonstrated by Ansalone et al, pacing in the area of latest activation results in the best clinical response compared to patients with the LV lead beyond the site of latest activation (98). Third, does the site of latest activation contain scar tissue? Recent observations showed that scar tissue in the region of the LV pacing lead resulted in CRT failure (71). But also the extent of scar tissue is important; Ypenburg et al observed that at least 11 viable LV segments (in a 16-segment model) are needed for a positive response to CRT (87). Fourth, is venous access present to the preferred location? MSCT can provide this information non-invasively (91). A surgical approach is preferred in case of absence of suitable cardiac veins.

Image-integration may answer all these questions at the same time. Goitein et al presented a method for integration of information provided by MSCT (venous anatomy) and echocardiography (LV dyssynchrony and site of latest activation) using commercially available software (99). The integrated image demonstrates an isochronal map of peak strain time derived from echocardiographic images, coronary venous anatomy, and approximate course of the left phrenic nerve (see Figure 19). These images can be used to evaluate the best LV lead position. Still, prospective large studies are needed comparing empiric and guided LV lead implantation (targeted at the site of latest activation).

In conclusion, various non-invasive imaging techniques may play a role in the selection of patients for CRT. Echocardiography still appears the technique of choice to assess LV dyssynchrony, whereas other imaging techniques may provide additional information on scar tissue and venous anatomy.

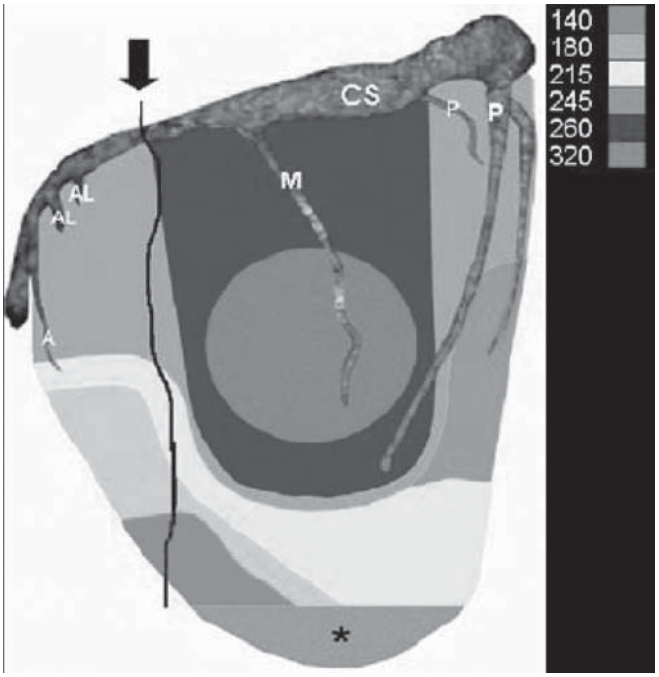

Figure 19. Image-integration

Integrated image demonstrating isochronal map of peak strain time derived from echocardiographic images (colorscale in ms referenced to QRS complex shown on right), coronary venous anatomomy, and approximate course of the left phrenic nerve. The gray region (*) could not be assayed echocardiographically because of transducer angulation limitations. CS: coronary sinus, M: marginal branch, P: posterior branch, A: anterior branch, AL: anterolateral branch. Adapted from Goitein et al (99).

REFERENCES

1. Auricchio A, Stellbrink C, Sack S et al. Long-term clinical effect of hemodynamically optimized cardiac resynchronization therapy in patients with heart failure and ventricular conduction delay. J Am Coll Cardiol 2002;39:2026-33.
2. Cazeau S, Leclercq C, Lavergne T et al. Effects of multisite biventricular pacing in patients with heart failure and intraventricular conduction delay. N Engl J Med 2001;344:873-80.
3. Abraham WT, Fisher WG, Smith AL et al. Cardiac resynchronization in chronic heart failure. N Engl J Med 2002;346:1845-53.
4. Young JB, Abraham WT, Smith AL et al. Combined cardiac resynchronization and implantable cardioversion defibrillation in advanced chronic heart failure: the MIRACLE ICD Trial. JAMA 2003;289:2685-94.
5. Bristow MR, Saxon LA, Boehmer J et al. Cardiac-resynchronization therapy with or without an implantable defibrillator in advanced chronic heart failure. N Engl J Med 2004;350:2140-50.
6. Cleland JG, Daubert JC, Erdmann E et al. The effect of cardiac resynchronization on morbidity and mortality in heart failure. N Engl J Med 2005;352:1539-49.
7. Strickberger SA, Conti J, Daoud EG et al. Patient selection for cardiac resynchronization therapy: from the Council on Clinical Cardiology Subcommittee on Electrocardiography and Arrhythmias and the Quality of Care and Outcomes Research Interdisciplinary Working Group, in collaboration with the Heart Rhythm Society. Circulation 2005;111:2146-50.
8. Bax JJ, Ansalone G, Breithardt OA et al. Echocardiographic evaluation of cardiac resynchronization therapy: ready for routine clinical use? A critical appraisal. J Am Coll Cardiol 2004;44:1-9.
9. Van Beeumen K, Duytschaever M, Tavernier R et al. Intra- and interatrial asynchrony in patients with heart failure. Am J Cardiol 2007;99:79-83.
10. Auricchio A, Fantoni C, Regoli F et al. Characterization of left ventricular activation in patients with heart failure and left bundle-branch block. Circulation 2004;109:1133-9.
11. Kashani A, Barold SS. Significance of QRS complex duration in patients with heart failure. J Am Coll Cardiol 2005;46:2183-92.
12. Penicka M, Bartunek J, De Bruyne B et al. Improvement of left ventricular function after cardiac resynchronization therapy is predicted by tissue Doppler imaging echocardiography. Circulation 2004;109:978-83.
13. Mollema SA, Bleeker GB, van der Wall EE et al. Usefulness of QRS Duration to Predict Response to Cardiac Resynchronization Therapy in Patients With End-Stage Heart Failure. Am J Cardiol 2007;100:1665-70.
14. Kurzidim K, Reinke H, Sperzel J et al. Invasive optimization of cardiac resynchronization therapy: role of sequential biventricular and left ventricular pacing. Pacing Clin Electrophysiol 2005;28:754-61.
15. Bleeker GB, Schalij MJ, Molhoek SG et al. Relationship between QRS duration and left ventricular dyssynchrony in patients with end-stage heart failure. J Cardiovasc Electrophysiol 2004;15:544-9.
16. Ghio S, Constantin C, Klersy C et al. Interventricular and intraventricular dyssynchrony are common in heart failure patients, regardless of QRS duration. Eur Heart J 2004;25:571-8.
17. Bleeker GB, Schalij MJ, Molhoek SG et al. Frequency of left ventricular dyssynchrony in patients with heart failure and a narrow QRS complex. Am J Cardiol 2005;95:140-2.
18. Yu CM, Lin H, Zhang Q et al. High prevalence of left ventricular systolic and diastolic asynchrony in patients with congestive heart failure and normal QRS duration. Heart 2003;89:54-60.
19. Bax JJ, Abraham T, Barold SS et al. Cardiac resynchronization therapy part 1-issues before device implantation. J Am Coll Cardiol 2005;46:2153-67.
20. Chung ES, Leon AR, Tavazzi L et al. Results of the Predictors of Response to CRT (PROSPECT) Trial. Circulation;117:2608-16.
21. Pitzalis MV, Iacoviello M, Romito R et al. Cardiac resynchronization therapy tailored by echocardiographic evaluation of ventricular asynchrony. J Am Coll Cardiol 2002;40:1615-22.
22. Marcus GM, Rose E, Viloria EM et al. Septal to posterior wall motion delay fails to predict reverse remodeling or clinical improvement in patients undergoing cardiac resynchronization therapy. J Am Coll Cardiol 2005;46:2208-14.

23. Bleeker GB, Schalij MJ, Boersma E et al. Relative merits of M-mode echocardiography and tissue Doppler imaging for prediction of response to cardiac resynchronization therapy in patients with heart failure secondary to ischemic or idiopathic dilated cardiomyopathy. Am J Cardiol 2007;99:68-74.
24. Cazeau S, Bordachar P, Jauvert G et al. Echocardiographic modeling of cardiac dyssynchrony before and during multisite stimulation: a prospective study. Pacing Clin Electrophysiol 2003;26:137-43.
25. Bordachar P, Lafitte S, Reuter S et al. Echocardiographic parameters of ventricular dyssynchrony validation in patients with heart failure using sequential biventricular pacing. J Am Coll Cardiol 2004;44:2157-65.
26. Achilli A, Peraldo C, Sassara M et al. Prediction of response to cardiac resynchronization therapy: the selection of candidates for CRT (SCART) study. Pacing Clin Electrophysiol 2006;29 Suppl 2:S11-S19.
27. Richardson M, Freemantle N, Calvert MJ et al. Predictors and treatment response with cardiac resynchronization therapy in patients with heart failure characterized by dyssynchrony: a pre-defined analysis from the CARE-HF trial. Eur Heart J 2007;28:1827-34.
28. Garrigue S, Reuter S, Labeque JN et al. Usefulness of biventricular pacing in patients with congestive heart failure and right bundle branch block. Am J Cardiol 2001;88:1436-41.
29. Ansalone G, Giannantoni P, Ricci R et al. Doppler myocardial imaging in patients with heart failure receiving biventricular pacing treatment. Am Heart J 2001;142:881-96.
30. Bax JJ, Marwick TH, Molhoek SG et al. Left ventricular dyssynchrony predicts benefit of cardiac resynchronization therapy in patients with end-stage heart failure before pacemaker implantation. Am J Cardiol 2003;92:1238-40.
31. Bax JJ, Bleeker GB, Marwick TH et al. Left ventricular dyssynchrony predicts response and prognosis after cardiac resynchronization therapy. J Am Coll Cardiol 2004;44:1834-40.
32. Yu CM, Chau E, Sanderson JE et al. Tissue Doppler echocardiographic evidence of reverse remodeling and improved synchronicity by simultaneously delaying regional contraction after biventricular pacing therapy in heart failure. Circulation 2002;105:438-45.
33. Yu CM, Fung WH, Lin H et al. Predictors of left ventricular reverse remodeling after cardiac resynchronization therapy for heart failure secondary to idiopathic dilated or ischemic cardiomyopathy. Am J Cardiol 2003;91:684-8.
34. Yu CM, Zhang Q, Chan YS et al. Tissue Doppler velocity is superior to displacement and strain mapping in predicting left ventricular reverse remodelling response after cardiac resynchronisation therapy. Heart 2006;92:1452-6.
35. Yu CM, Fung JW, Zhang Q et al. Tissue Doppler imaging is superior to strain rate imaging and postsystolic shortening on the prediction of reverse remodeling in both ischemic and nonischemic heart failure after cardiac resynchronization therapy. Circulation 2004;110:66-73.
36. Yu CM, Gorcsan J, III, Bleeker GB et al. Usefulness of tissue Doppler velocity and strain dyssynchrony for predicting left ventricular reverse remodeling response after cardiac resynchronization therapy. Am J Cardiol 2007;100:1263-70.
37. Notabartolo D, Merlino JD, Smith AL et al. Usefulness of the peak velocity difference by tissue Doppler imaging technique as an effective predictor of response to cardiac resynchronization therapy. Am J Cardiol 2004;94:817-20.
38. Knebel F, Schattke S, Bondke H et al. Evaluation of longitudinal and radial two-dimensional strain imaging versus Doppler tissue echocardiography in predicting long-term response to cardiac resynchronization therapy. J Am Soc Echocardiogr 2007;20:335-41.
39. Van de Veire NR, Yu CM, Ajmone Marsan N et al. Tri-plane Tissue Doppler Imaging: a novel 3-dimensional imaging modality that predicts reverse left ventricular remodeling after Cardiac Resynchronization Therapy. Heart 2008;94:e9.
40. Van de Veire NR, Bleeker GB, De Sutter J et al. Tissue synchronisation imaging accurately measures left ventricular dyssynchrony and predicts response to cardiac resynchronisation therapy. Heart 2007;93:1034-9.
41. Popovic ZB, Grimm RA, Perlic G et al. Noninvasive assessment of cardiac resynchronization therapy for congestive heart failure using myocardial strain and left ventricular peak power as parameters of myocardial synchrony and function. J Cardiovasc Electrophysiol 2002;13:1203-8.

42. Hashimoto I, Li X, Hejmadi BA et al. Myocardial strain rate is a superior method for evaluation of left ventricular subendocardial function compared with tissue Doppler imaging. J Am Coll Cardiol 2003;42:1574-83.

43. Dohi K, Suffoletto MS, Schwartzman D et al. Utility of echocardiographic radial strain imaging to quantify left ventricular dyssynchrony and predict acute response to cardiac resynchronization therapy. Am J Cardiol 2005;96:112-6.

44. Sogaard P, Kim WY, Jensen HK et al. Impact of acute biventricular pacing on left ventricular performance and volumes in patients with severe heart failure. A tissue doppler and three-dimensional echocardiographic study. Cardiology 2001;95:173-82.

45. Sogaard P, Egeblad H, Kim WY et al. Tissue Doppler imaging predicts improved systolic performance and reversed left ventricular remodeling during long-term cardiac resynchronization therapy. J Am Coll Cardiol 2002;40:723-30.

46. Sogaard P, Egeblad H, Pedersen AK et al. Sequential versus simultaneous biventricular resynchronization for severe heart failure: evaluation by tissue Doppler imaging. Circulation 2002;106:2078-84.

47. Suffoletto MS, Dohi K, Cannesson M et al. Novel speckle-tracking radial strain from routine black-and-white echocardiographic images to quantify dyssynchrony and predict response to cardiac resynchronization therapy. Circulation 2006;113:960-8.

48. Becker M, Kramann R, Franke A et al. Impact of left ventricular lead position in cardiac resynchronization therapy on left ventricular remodelling. A circumferential strain analysis based on 2D echocardiography. Eur Heart J 2007;28:1211-20.

49. Gorcsan J, III, Tanabe M, Bleeker GB et al. Combined longitudinal and radial dyssynchrony predicts ventricular response after resynchronization therapy. J Am Coll Cardiol 2007;50:1476-83.

50. Delgado V, Ypenburg C, van Bommel RJ et al. Assessment of left ventricular dyssynchrony by speckle tracking strain imaging comparison between longitudinal, circumferential, and radial strain in cardiac resynchronization therapy. J Am Coll Cardiol 2008;51:1944-52.

51. Cannesson M, Tanabe M, Suffoletto MS et al. Velocity vector imaging to quantify ventricular dyssynchrony and predict response to cardiac resynchronization therapy. Am J Cardiol 2006;98:949-53.

52. Kapetanakis S, Kearney MT, Siva A et al. Real-time three-dimensional echocardiography: a novel technique to quantify global left ventricular mechanical dyssynchrony. Circulation 2005;112:992-1000.

53. Zhang Q, Fung JW, Auricchio A et al. Differential change in left ventricular mass and regional wall thickness after cardiac resynchronization therapy for heart failure. Eur Heart J 2006;27:1423-30.

54. Ajmone Marsan N, Bleeker GB, Ypenburg C et al. Real-Time Three-Dimensional Echocardiography Permits Quantification of Left Ventricular Mechanical Dyssynchrony and Predicts Acute Response to Cardiac Resynchronization Therapy. J Cardiovasc Electrophysiol 2008;19:392-9.

55. Mele D, Pasanisi G, Capasso F et al. Left intraventricular myocardial deformation dyssynchrony identifies responders to cardiac resynchronization therapy in patients with heart failure. Eur Heart J 2006;27:1070-8.

56. Tada H, Toide H, Okaniwa H et al. Maximum Ventricular Dyssynchrony Predicts Clinical Improvement and Reverse Remodeling during Cardiac Resynchronization Therapy. Pacing Clin Electrophysiol 2007;30 Suppl 1:S13-S18.

57. Porciani MC, Lilli A, Macioce R et al. Utility of a new left ventricular asynchrony index as a predictor of reverse remodelling after cardiac resynchronization therapy. Eur Heart J 2006;27:1818-23.

58. van Rossum AC, Visser FC, Van Eenige MJ et al. Oblique views in magnetic resonance imaging of the heart by combined axial rotations. Acta Radiol 1987;28:497-503.

59. Lardo AC, Abraham TP, Kass DA. Magnetic resonance imaging assessment of ventricular dyssynchrony: current and emerging concepts. J Am Coll Cardiol 2005;46:2223-8.

60. Leclercq C, Faris O, Tunin R et al. Systolic improvement and mechanical resynchronization does not require electrical synchrony in the dilated failing heart with left bundle-branch block. Circulation 2002;106:1760-3.

61. Helm RH, Leclercq C, Faris OP et al. Cardiac dyssynchrony analysis using circumferential versus longitudinal strain: implications for assessing cardiac resynchronization. Circulation 2005;111:2760-7.

62. Zwanenburg JJ, Gotte MJ, Kuijer JP et al. Timing of cardiac contraction in humans mapped by high-temporal-resolution MRI tagging: early onset and late peak of shortening in lateral wall. Am J Physiol Heart Circ Physiol 2004;286:H1872-H1880.

63. Zwanenburg JJ, Gotte MJ, Marcus JT et al. Propagation of onset and peak time of myocardial shortening in time of myocardial shortening in ischemic versus nonischemic cardiomyopathy: assessment by magnetic resonance imaging myocardial tagging. J Am Coll Cardiol 2005;46:2215-22.

64. Pelc NJ, Herfkens RJ, Shimakawa A et al. Phase contrast cine magnetic resonance imaging. Magn Reson Q 1991;7:229-54.

65. Westenberg JJ, Lamb HJ, van der Geest RJ et al. Assessment of left ventricular dyssynchrony in patients with conduction delay and idiopathic dilated cardiomyopathy: head-to-head comparison between tissue doppler imaging and velocity-encoded magnetic resonance imaging. J Am Coll Cardiol 2006;47:2042-8.

66. Delfino JG, Bhasin M, Cole R et al. Comparison of myocardial velocities obtained with magnetic resonance phase velocity mapping and tissue Doppler imaging in normal subjects and patients with left ventricular dyssynchrony. J Magn Reson Imaging 2006;24:304-11.

67. Markl M, Schneider B, Hennig J. Fast phase contrast cardiac magnetic resonance imaging: improved assessment and analysis of left ventricular wall motion. J Magn Reson Imaging 2002;15:642-53.

68. van der Geest RJ, Reiber JH. Quantification in cardiac MRI. J Magn Reson Imaging 1999;10:602-8.

69. Kaandorp TA, Lamb HJ, van der Wall EE et al. Cardiovascular MR to access myocardial viability in chronic ischaemic LV dysfunction. Heart 2005;91:1359-65.

70. Kim RJ, Fieno DS, Parrish TB et al. Relationship of MRI delayed contrast enhancement to irreversible injury, infarct age, and contractile function. Circulation 1999;100:1992-2002.

71. Bleeker GB, Kaandorp TA, Lamb HJ et al. Effect of posterolateral scar tissue on clinical and echocardiographic improvement after cardiac resynchronization therapy. Circulation 2006;113:969-76.

72. White JA, Yee R, Yuan X et al. Delayed enhancement magnetic resonance imaging predicts response to cardiac resynchronization therapy in patients with intraventricular dyssynchrony. J Am Coll Cardiol 2006;48:1953-60.

73. Ypenburg C, Roes SD, Bleeker GB et al. Effect of total scar burden on contrast-enhanced magnetic resonance imaging on response to cardiac resynchronization therapy. Am J Cardiol 2007;99:657-60.

74. Nezafat R, Han Y, Peters DC et al. Coronary magnetic resonance vein imaging: imaging contrast, sequence, and timing. Magn Reson Med 2007;58:1196-206.

75. Rasche V, Binner L, Cavagna F et al. Whole-heart coronary vein imaging: a comparison between non-contrast-agent- and contrast-agent-enhanced visualization of the coronary venous system. Magn Reson Med 2007;57:1019-26.

76. Chiribiri A, Kelle S, Gotze S et al. Visualization of the cardiac venous system using cardiac magnetic resonance. Am J Cardiol 2008;101:407-12.

77. Zimmermann BH, Faul DD. Artifacts and hazards in NMR imaging due to metal implants and cardiac pacemakers. Diagn Imaging Clin Med 1984;53:53-6.

78. Roguin A, Zviman MM, Meininger GR et al. Modern pacemaker and implantable cardioverter/defibrillator systems can be magnetic resonance imaging safe: in vitro and in vivo assessment of safety and function at 1.5 T. Circulation 2004;110:475-82.

79. Botvinick EH. Scintigraphic blood pool and phase image analysis: the optimal tool for the evaluation of resynchronization therapy. J Nucl Cardiol 2003;10:424-8.

80. O'Connell JW, Schreck C, Moles M et al. A unique method by which to quantitate synchrony with equilibrium radionuclide angiography. J Nucl Cardiol 2005;12:441-50.

81. Kerwin WF, Botvinick EH, O'Connell JW et al. Ventricular contraction abnormalities in dilated cardiomyopathy: effect of biventricular pacing to correct interventricular dyssynchrony. J Am Coll Cardiol 2000;35:1221-7.

82. Toussaint JF, Lavergne T, Kerrou K et al. Basal asynchrony and resynchronization with biventricular pacing predict long-term improvement of LV function in heart failure patients. Pacing Clin Electrophysiol 2003;26:1815-23.

83. Chen J, Garcia EV, Folks RD et al. Onset of left ventricular mechanical contraction as determined by phase analysis of ECG-gated myocardial perfusion SPECT imaging: development of a diagnostic tool for assessment of cardiac mechanical dyssynchrony. J Nucl Cardiol 2005;12:687-95.
84. Henneman MM, Chen J, Ypenburg C et al. Phase analysis of gated myocardial perfusion single-photon emission computed tomography compared with tissue Doppler imaging for the assessment of left ventricular dyssynchrony. J Am Coll Cardiol 2007;49:1708-14.
85. Henneman MM, Chen J, Dibbets-Schneider P et al. Can LV Dyssynchrony as Assessed with Phase Analysis on Gated Myocardial Perfusion SPECT Predict Response to CRT? J Nucl Med 2007;48:1104-11.
86. Sciagra R, Giaccardi M, Porciani MC et al. Myocardial perfusion imaging using gated SPECT in heart failure patients undergoing cardiac resynchronization therapy. J Nucl Med 2004;45:164-8.
87. Ypenburg C, Schalij MJ, Bleeker GB et al. Extent of viability to predict response to cardiac resynchronization therapy in ischemic heart failure patients. J Nucl Med 2006;47:1565-70.
88. Ypenburg C, Schalij MJ, Bleeker GB et al. Impact of viability and scar tissue on response to cardiac resynchronization therapy in ischaemic heart failure patients. Eur Heart J 2007;28:33-41.
89. Adelstein EC, Saba S. Scar burden by myocardial perfusion imaging predicts echocardiographic response to cardiac resynchronization therapy in ischemic cardiomyopathy. Am Heart J 2007;153:105-12.
90. Meisel E, Pfeiffer D, Engelmann L et al. Investigation of coronary venous anatomy by retrograde venography in patients with malignant ventricular tachycardia. Circulation 2001;104:442-7.
91. Jongbloed MR, Lamb HJ, Bax JJ et al. Noninvasive visualization of the cardiac venous system using multislice computed tomography. J Am Coll Cardiol 2005;45:749-53.
92. Van de Veire NR, Schuijf JD, De Sutter J et al. Non-invasive visualization of the cardiac venous system in coronary artery disease patients using 64-slice computed tomography. J Am Coll Cardiol 2006;48:1832-8.
93. Auricchio A, Sorgente A, Singh JP et al. Role of multislice computed tomography for preprocedural evaluation before revision of a chronically implanted transvenous left ventricular lead. Am J Cardiol 2007;100:1566-70.
94. Henneman MM, Schuijf JD, Jukema JW et al. Comprehensive cardiac assessment with multislice computed tomography: evaluation of left ventricular function and perfusion in addition to coronary anatomy in patients with previous myocardial infarction. Heart 2006;92:1779-83.
95. Rist C, Johnson TR, Becker CR et al. New applications for noninvasive cardiac imaging: dual-source computed tomography. Eur Radiol 2007;17 Suppl 6:F16-F25.
96. Jia P, Ramanathan C, Ghanem RN et al. Electrocardiographic imaging of cardiac resynchronization therapy in heart failure: observation of variable electrophysiologic responses. Heart Rhythm 2006;3:296-310.
97. Varma N, Jia P, Rudy Y. Electrocardiographic imaging of patients with heart failure with left bundle branch block and response to cardiac resynchronization therapy. J Electrocardiol 2007;40:S174-S178.
98. Ansalone G, Giannantoni P, Ricci R et al. Doppler myocardial imaging to evaluate the effectiveness of pacing sites in patients receiving biventricular pacing. J Am Coll Cardiol 2002;39:489-99.
99. Goitein O, Lacomis JM, Gorcsan J, III et al. Left ventricular pacing lead implantation: potential utility of multimodal image integration. Heart Rhythm 2006;3:91-4.
100. Gasparini M, Lunati M, Bocchiardo M et al. Cardiac resynchronization and implantable cardioverter defibrillator therapy: preliminary results from the InSync Implantable Cardioverter Defibrillator Italian Registry. Pacing Clin Electrophysiol 2003;26:148-51.
101. Higgins SL, Hummel JD, Niazi IK et al. Cardiac resynchronization therapy for the treatment of heart failure in patients with intraventricular conduction delay and malignant ventricular tachyarrhythmias. J Am Coll Cardiol 2003;42:1454-9.
102. Molhoek SG, Bax JJ, Bleeker GB et al. Long-term follow-up of cardiac resynchronization therapy in patients with end-stage heart failure. J Cardiovasc Electrophysiol 2005;16:701-7.
103. Bleeker GB, Schalij MJ, Molhoek SG et al. Comparison of effectiveness of cardiac resynchronization therapy in patients <70 versus > or =70 years of age. Am J Cardiol 2005;96:420-2.
104. Leon AR, Abraham WT, Brozena S et al. Cardiac resynchronization with sequential biventricular pacing for the treatment of moderate-to-severe heart failure. J Am Coll Cardiol 2005;46:2298-304.

105. Bleeker GB, Schalij MJ, Boersma E et al. Does a gender difference in response to cardiac resynchronization therapy exist? Pacing Clin Electrophysiol 2005;28:1271-5.

106. Boriani G, Saporito D, Biffi M et al. Acute and chronic haemodynamic effects of biventricular pacing and of switching to different pacing modalities in heart failure patients. Int J Cardiol 2006;110:318-23.

107. Bleeker GB, Bax JJ, Fung JW et al. Clinical versus echocardiographic parameters to assess response to cardiac resynchronization therapy. Am J Cardiol 2006;97:260-3.

108. Ypenburg C, van Erven L, Bleeker GB et al. Benefit of combined resynchronization and defibrillator therapy in heart failure patients with and without ventricular arrhythmias. J Am Coll Cardiol 2006;48:464-70.

109. Pires LA, Abraham WT, Young JB et al. Clinical predictors and timing of New York Heart Association class improvement with cardiac resynchronization therapy in patients with advanced chronic heart failure: results from the Multicenter InSync Randomized Clinical Evaluation (MIRACLE) and Multicenter InSync ICD Randomized Clinical Evaluation (MIRACLE-ICD) trials. Am Heart J 2006;151:837-43.

110. Yeim S, Bordachar P, Reuter S et al. Predictors of a positive response to biventricular pacing in patients with severe heart failure and ventricular conduction delay. Pacing Clin Electrophysiol 2007;30:970-5.

111. Lellouche N, De Diego C, Cesario DA et al. Usefulness of preimplantation B-type natriuretic peptide level for predicting response to cardiac resynchronization therapy. Am J Cardiol 2007;99:242-6.

112. Yu CM, Bleeker GB, Fung JW et al. Left ventricular reverse remodeling but not clinical improvement predicts long-term survival after cardiac resynchronization therapy. Circulation 2005;112:1580-6.

113. Yu CM, Zhang Q, Fung JW et al. A novel tool to assess systolic asynchrony and identify responders of cardiac resynchronization therapy by tissue synchronization imaging. J Am Coll Cardiol 2005;45:677-84.

114. Murphy RT, Sigurdsson G, Mulamalla S et al. Tissue synchronization imaging and optimal left ventricular pacing site in cardiac resynchronization therapy. Am J Cardiol 2006;97:1615-21.

115. Jansen AH, Bracke F, van Dantzig JM et al. Optimization of pulsed wave tissue Doppler to predict left ventricular reverse remodeling after cardiac resynchronization therapy. J Am Soc Echocardiogr 2006;19:185-91.

116. Yu CM, Zhang Q, Yip GW et al. Are left ventricular diastolic function and diastolic asynchrony important determinants of response to cardiac resynchronization therapy? Am J Cardiol 2006;98:1083-7.

117. Jansen AH, Bracke F, Dantzig JM et al. The influence of myocardial scar and dyssynchrony on reverse remodeling in cardiac resynchronization therapy. Eur J Echocardiogr 2008;9:483-8.

118. Fung JW, Chan JY, Kum LC et al. Suboptimal medical therapy in patients with systolic heart failure is associated with less improvement by cardiac resynchronization therapy. Int J Cardiol 2007;115:214-9.

119. Yu CM, Fang F, Zhang Q et al. Improvement of atrial function and atrial reverse remodeling after cardiac resynchronization therapy for heart failure. J Am Coll Cardiol 2007;50:778-85.

120. Fung JW, Szeto CC, Chan JY et al. Prognostic value of renal function in patients with cardiac resynchronization therapy. Int J Cardiol 2007;122:10-6.

121. Pitzalis MV, Iacoviello M, Romito R et al. Ventricular asynchrony predicts a better outcome in patients with chronic heart failure receiving cardiac resynchronization therapy. J Am Coll Cardiol 2005;45:65-9.

122. Diaz-Infante E, Sitges M, Vidal B et al. Usefulness of ventricular dyssynchrony measured using M-mode echocardiography to predict response to resynchronization therapy. Am J Cardiol 2007;100:84-9.

123. Van de Veire NR, Bleeker GB, Ypenburg C et al. Usefulness of triplane tissue Doppler imaging to predict acute response to cardiac resynchronization therapy. Am J Cardiol 2007;100:476-82.

124. Gorcsan J, III, Kanzaki H, Bazaz R et al. Usefulness of echocardiographic tissue synchronization imaging to predict acute response to cardiac resynchronization therapy. Am J Cardiol 2004;93:1178-81.